Powerful solution for experimental cerebral malaria treatment: artesunate and tetramethylpyrazine

Xiaohui Jiang[+, 1, 2], Lina Chen[+, 1, 2], Zhongyuan Zheng[1, 2]; Yuan Guo[1, 2]; Kai Li[1, 2]; Ying Chen[2]; Xiaogang Weng[2]; Ting Yang[1, 2]; Shuiqing Qu[1, 2]; Hui Liu[1, 2]; Yujie Li[*, 1, 2]; Xiaoxin Zhu[*, 1, 2]

1 Artemisinin Research Center, China Academy of Chinese Medical Sciences, No. 16 Dongzhimen Nei Avenue, Beijing, 100700, China

2 Institute of Chinese Materia Medica, China Academy of Chinese Medical Sciences, No. 16 Dongzhimen Nei Avenue, Beijing, 100700, China

[+]These authors contributed equally to this article.

*Correspondence:

Xiaohui Jiang : 2532253990@qq.com

Lina Chen : lnchen@icmm.ac.cn

Zhongyuan Zheng : zhengzhongyuan89757@126.com

Yuan Guo : guoyuanm@163.com

Kai Li : likaityki@163.com

Ying Chen: chenying919@126.com

Xiaogang Weng: xgweng75@126.com

Ting Yang: 18435148439@163.com

Shuiqing Qu: 1272086206@qq.com

Hui Liu: 15871421085@163.com

Yujie Li : yjli@icmm.ac.cn

Xiaoxin Zhu : xxzhu@icmm.ac.cn

Abstract

Background: Cerebral malaria (CM) is a kind of serious neurological complication caused by the acute Plasmodium falciparum infection. About 300000 patients including children under 5 years old died from this disease every year. Even intravenous artesunate (Art) is employed as the most effictive drug in the treatment of CM, high incidence of death and neurological sequelae are still inevitable. Therefore, we assessed the combination of Art and tetramethylpyrazine (TMP), to treat experimental CM (ECM) in C57BL/6 mice infected with *Plasmodium berghei* ANKA (PbA). A non-biased whole brain quantitative proteomic analysis was also conducted to get some insight of the mechanism of the combinational treatment.

Results: Treatment of (ECM)-C57BL/6 mice with the combination of Art and TMP increased the survival, improved clinical signs and prevented neurological manifestations. These effects were related to reduction of parasitised red blood cells (pRBC) adhesion, sequestration, maintaining brain microvascular integrity, increasing nerve growth factor, neurotrophin levels, and alleviating hippocampal neuronal damage and astrocyte activation. The pharmacological effects of Art-TMP combination therapy were analyzed by ECM mice brain proteomic function enrichment. Based on an isobaric tag for relative and absolute quantitation (iTRAQ) fold-change of 1.2 (P-value < 0.05), 217 down-regulated and 177 up-regulated proteins were identified, presenting a significantly altered proteome profile of the combined Art and TMP group as compared to the group treated with Art or TMP alone. These results suggested that the Art-TMP combination could be used as a

powerful solution for CM and its neurologic damage.

Conclusions: An effictive therapy for CM with low mortality rate and protect against ECM-induced neurocognitive impairment has been proposed through the combination of Art and TMP, which can provide an effective adjuvant treatment in the clinic. iTRAQ proteomics provide a resource for further mechanistic studies to examine the synergistic effects of Art and TMP and their potential to serve as an adjunctive treatment method and intervention targets.

Key words: Artesunate, Tetramethylpyrazine, Cerebral malaria, Neurological sequelae，Outcome, Quantitative proteomics

Author Summary

Cerebral malaria (CM) is the most serious neurological complication caused by Plasmodium falciparum infection. Even after antimalarial treatment, severe neurological sequelae still exist. We used tetramethylpyrazine (TMP), the main ingredient of the traditional Chinese medicine Chuanxiong, and artesunate (Art) as a combination of drugs. We found that Art-TMP combination could improve the clinical symptoms of CM and protect the nervous system. At the same time, proteomics was used to analyze the protective mechanism of Art-TMP combination administration on ECM mice. This study suggests that the combination of Art and TMP may be used as an adjuvant therapy for clinical CM and iTRAQ proteomics provides resources for further study of Art-TMP combination and provides potential prognostic biomarkers for this therapeutic intervention.

Introduction

Malaria is considered to be one of the world's three major infectious diseases that resulted in the death of 435,000 people in 2017. According to the 2018 World Malaria Report, 61% of all deaths due to malaria occurred in children under the age of five years [1]. Cerebral malaria (CM) is one of the major complications of *Plasmodium falciparum* infection. It is associated with severe disturbances of the consciousness (deep coma) and respiratory distress or other neurological abnormalities [2]. The World Health Organization (WHO) has recommended intravenous Art as the first-line treatment for severe malaria. Moreover, the therapeutic effects of intravenous Art are superior to those of quinine [3, 4]. However, Art monotherapy is insufficient to control the mortality rate, owing to a lack of specific neuro- and vasculo-protective effects, leading to approximately 300,000 deaths each year. Furthermore, about 26% of individuals present neurological deficits, such as learning and memory deficits, and language disability despite being administered anti-malarial drugs [5, 6]. Moreover, intravenous administration is largely restricted to the high-risk areas of malaria in Africa, CM remains a dominant cause of mortality and neurodisability in the tropics. As a consequence, there is an urgent clinical need to develop more effective and robust treatments for CM, with an aim to improve the protective effects of anti-malarial drugs.

Literature regarding the cerebral processes involved in the pathogenesis of CM

and those that undermine the recovery from the complication after anti-malarial drug therapy is scarce. However, there is an increasing consensus that protecting the host brain vascular system and neurons and modulating the host pro-inflammatory immune response to infection are plausible effective strategies to improve the success of the anti-malarial drug therapy of CM. Indeed, vascular obstruction and immunopathology are known to be generally associated with the life-threatening symptoms of CM, which may interrupt the recovery by activating endothelial cells, astrocytes, and microglial cells in the brain, thereby disrupting the blood–brain barrier integrity, disturbing and/or destroying neuronal signalling and causing nerve injuries [7, 8]. All these abnormalities have been observed in the brains of patients with CM. It is believed that a dysfunction of blood vessels in the brain is the primary cause of development of CM, which may prevent the re-establishment of brain homeostasis, leading to the failure of the anti-malarial drug treatment.

To improve the fatal outcome caused by CM, the need of the hour is to explore a novel, inexpensive adjunctive therapy that can be easily administered and can improve neurological sequelae. Although Chuanxiong is not a major therapeutic medicine for malaria, several reports on the prescription of Chuanxiong as a combination therapy for malaria exist in the classical literature, such as nasal plug of Chuanxiong for malaria in Mongolian medicine. Tetramethylpyrazine (TMP) is the primary active alkaloid component of the traditional Chinese medicine Chuanxiong. Its use to treat cerebrovascular diseases could be traced back to thousands of years ago; moreover, it is known to exert protective effects on various nervous system

111 injuries [9, 10]. TMP has been demonstrated to increase cerebral blood flow, improve
112 microcirculation, inhibit the production of pro-inflammatory factors and protect
113 learning and memory functions [11, 12]. Recently, clinical studies have reported that
114 TMP exerts beneficial effects on the nervous system that can promote functional
115 recovery from nerve injury. Adjunctive therapy is defined as an additional treatment
116 that modifies the pathological processes caused by malaria to improve its clinical
117 outcomes and/or decline mortality, along with the prevention of long-term
118 neurocognitive impairment [13]. Over the past decades, dozens of CM interventions
119 for different pathways have been evaluated based on immunomodulation,
120 neuroprotection, regulation of gaseous signalling molecules and improvement of
121 endothelial dysfunction [14]. In fact, more than 17 clinical trials have so far examined
122 11 treatments; however, no method has been proven effective in treating CM in
123 children [15, 16].

124 The present study aimed to find an adjunctive therapy to improve neurological
125 symptoms and survival in an experimental cerebral malaria (ECM) model. C57BL/6
126 mice were infected with *Plasmodium berghei* ANKA (PbA) and treated daily with
127 Art, TMP, and a combination of Art and TMP. Parasitaemia and clinical, histological,
128 and immunological features of the disease were monitored. Subsequently, to elucidate
129 possible targets of Art-TMP combination in treating ECM, we performed an extensive
130 quantitative proteomic analysis to compare the brain proteome profiles of ECM mice
131 treated with Art, TMP, and Art-TMP combination with those of ECM model control
132 mice. Interestingly, certain brain proteins, such as Slit2, Tiam2, Syntenin, and

Hemopexin, were found to be sequentially altered in mice treated with the Art-TMP combination as compared to the proteins in the ECM mice. Here, we present the first comprehensive brain proteomic analysis of ECM mice treated with different drug combinations.

Materials and Methods

Ethics Statement

All experiments were carried out to minimize the suffering of animals. The care of laboratory animal and the animal experimental operation have conforming to Beijing Administration Rule of Laboratory Animal. All animal experiments were approved by the Animal Experimental Ethics Review Committee of the Institute of Basic Research for Chinese Medicine, China Academy of Chinese Medical Sciences (license number: SYXK (Beijing) 2016-0021).

Mice, parasitic infection, and disease assessment

Six- to eight-week-old male C57BL/6 mice weighing 14 to 16 g were purchased from the National Institutes for Food and Drug control (Beijing, China). *P. berghei* ANKA, originally obtained from Dr. Ya Zhao at the Fourth Military Medical University, was passaged *in vivo*. Experimental mice were infected with 1×10^6 parasitised red blood cells (pRBC) via intraperitoneal (i.p.) injection (recorded as day 0 [d0] post infection [p.i.]). Parasitaemia was monitored every day using Giemsa-stained blood smears. When mice develop reduced responsiveness to external stimuli, ataxia, paralysis or coma and convulsions are considered as typical symptoms

of ECM [17].

Treatment and drug administration

Experimental mice were randomised into four groups: PbA-infected group (Infected); artesunate (Art)-treated group; tetramethylpyrazine (TMP)-treated group and Art-TMP combination (Art+TMP)-treated group. Mice were treated with intranasal administration (IN) of 13.00 $mg \cdot kg^{-1}$ artesunate in the Art group, with ligustrazine hydrochloride injection (10.40 $mg \cdot kg^{-1}$) in the TMP group, and with Art-TMP combination (23.40 $mg \cdot kg^{-1}$) in the Art+TMP group, daily, starting from d2 till d5 p.i..

Basic indicator evaluation

To evaluate the effect of drugs on mice, survival rate (SR), body weight and body temperature were measured. Parasitaemia was monitored using the Giemsa-stained blood smears, and clinical symptoms of the diseased mice were evaluated using the rapid murine coma and behaviour scale (RMCBS) from d3 p.i. The RMCBS consists of 10 parameters (gait, balance, motor performance, body position, limb strength, touch escape, pinna reflex, toe pinch, aggression and grooming). Each parameter is scored 0 to 2, with a 0 score correlating with the lowest function and a 2 score correlating with the highest [18]. The lower the score, the worse the state of the mouse, thus indicating severity of the disease.

The open field test

We used the open field test to observe the spontaneous activity characteristics of mice entering a new environment [19]. Here, we used normal mice of the same age as

177 control. Briefly, mice were placed in four drums of an empty field activity test box (an
178 area with a central radius of 7.5 cm in a barrel is considered as the central area). Mice
179 were placed in the empty field and spontaneous activities of the animals were
180 observed within 5 minutes and recorded by the software automatically.

181 **Y-maze spontaneous alternation test**

182 Spontaneous alternation in the Y-maze was performed as previously described
183 [20]. A computer-controlled infrared camera system was installed directly above the
184 Y maze to track the location of mice. Animals were placed in a fixed position of the Y
185 maze in turn and allowed to explore freely for 8 minutes; normal mice were also used
186 as a control. The total number of entries into each arm was recorded during the
187 experiment.

188 **Histopathology and immunohistochemistry**

189 Six mice in each group were killed at 7 d p.i. Tissues were stained with
190 haematoxylin and eosin (H&E) for detecting microvascular obstructions.
191 Immunohistochemical staining was performed with specific polyclonal antibodies
192 against intercellular adhesion molecule-1 (ICAM-1), vascular cell adhesion
193 molecule-1 (VCAM-1), glial fibrillary acidic protein (GFAP) and neuron-specific
194 nuclear protein (NeuN) to detect the protein expression. Vessels were counted in 20
195 randomly selected fields per mouse using the method described in the literature [21].
196 GFAP-immunopositive cells in the cerebral cortex and NeuN-immunopositive cells in
197 the hippocampus were quantified in each mouse brain and counted in five areas per
198 section. The averaged data were used to evaluate the infiltration of inflammatory cells

199 into viable the neural tissue and to detect viability of neurons.

200 **Assessment of vessel integrity and patency by magnetic resonance imaging**

201 Mice in four groups were imaged at d7 p.i. using the following protocol. Each
202 mouse was anesthetised with 2,2,2-tribromoethanol (0.32 mg/kg^{-1}). Vessel integrity
203 and patency was scanned using TOF-2D-FLASH employing a magnetic resonance
204 imaging [MRI] scanner (BioSpec70/20 USR; Bruker, Germany) with the following
205 parameters: flip angle = 50 degrees, field of view = 20 × 20 cm^2, acquisition matrix
206 size = 256 × 256, slices = 0.5 mm, repetition time = 10 ms, echo time = 1.84 ms,
207 number of excitations = 5, imaging time = 6 minutes 49 seconds.

208 **Cytokine antibody arrays**

209 A panel of mouse cytokines was assessed by determining their relative levels of
210 expression using the RayBio® Cytokine Antibody Arrays (RayBiotech; Guangzhou,
211 China). In brief, 24 brain tissue samples were lysed and adjusted to a final
212 concentration of 500 μg/mL. Next, the cytokine antibody array was applied according
213 to the manufacturer's protocol. Intensities of fluorescent signals of the microarray
214 were measured using a laser microarray scanner (InnoScan 300 Microarray Scanner ;
215 Innopsys; France) at 532 nm and quantified using the RayBio® Analysis tool
216 software.

217 **Measurement of cytokine by enzyme-linked immunosorbent assay**

218 The levels of cytokines including brain-derived neurotrophic factor (BDNF),
219 neurotrophic factor-3 (NT-3) and tumour necrosis factor (TNF-α) were determined in
220 the mice brain using commercial enzyme-linked immunosorbent assay (ELISA) kits

as per the manufacturer's protocol. The absorbance value was measured at 450 nmusing the Thermo Mulitskan MK3 microplate. The concentration of each neurotrophic factor in every sample was calculated via a standard curve generated using recombinant cytokines. Data are represented as mean ± SEM from six animals in each group.

iTRAQ-based quantitative proteomic analyses

Specific methods of iTRAQ-based quantitative proteomic analyses were conducted using a method similar to that described in the literature [22]. In brief, the sample was lysed[23] followed by homogenisation; proteins in the sample were run on a sodium dodecyl sulphate polyacrylamide gel electrophoresis. The run sample was subjected to filter-aided sample preparation digestion, iTRAQ labelling, peptide fractionation using strong cation exchange chromatography, followed by HPLC and LC-MS/MS and data analyses.

Functional enrichment analysis

To further explore the impact of differentially expressed proteins and discover the internal relations between them, an enrichment analysis was performed. GO enrichment on three ontologies (biological processes, molecular functions, and cellular components) and the KEGG pathway enrichment were applied using Fisher's exact test, considering the whole quantified protein annotations as the background dataset. Benjamini–Hochberg correction for multiple testing was further applied to adjust the derived P-values. Only functional categories and pathways with P-values under a threshold of 0.05 are considered significant. The protein–protein interaction

243 information of the studied proteins was retrieved using the STRING software
244 (http://string-db.org/).

245 **Immunoblot analysis**

246 Proteomic results were confirmed by western blotting using the BIORAD system or
247 simple western analysis using the Wes™ protocol according to the manufacturer's
248 (Protein Simple Biosciences & Technology, USA) protocol. All primary antibodies
249 were used under the same condition (1:1000 dilution). For western blot analysis, the
250 lysed protein was denatured, followed by loading of the same amount of protein of
251 each mouse. The sample was electrophoresed, transferred, blocked, and incubated
252 with rabbit anti-mouse primary antibody overnight at 4°C. The sample was then
253 incubated with a secondary antibody at room temperature for 2 hours, after which
254 enhanced chemiluminescence (ECL) chromogen was added, the blot was scanned and
255 analysed in a gel-imaging system with actin as the internal reference.

256 For simple western analysis by Wes™, brain homogenate samples were prepared,
257 and protein concentration was determined using the bicinchoninic acid kit. The brain
258 homogenate samples were diluted to a final concentration of 1 μg/μL as required by
259 Wes™. Capillary electrophoresis immunoassay was performed using Wes-specific
260 reagent, 12–230 kDa Wes separation module 8 × 25 capillary filter. Electrophoresis
261 images were generated using the Protein Simple Compass software.

262 **Nasal administration toxicity study**

263 Toxicity study of nasal administration (NA) was assessed by histopathology of
264 the nasal mucosa. Nine healthy C57BL/6 mice were administered a placebo solution

or a mixed solution of injectable Art and ligustrazine hydrochloride injection (20 $mg \cdot kg^{-1}$) nasally. Three control mice and three mice administered drugs were sacrificed 30 minutes later. The other three mice were sacrificed 4 days after the intranasal administration of a mixture of injectable Art and ligustrazine hydrochloride injection (20 $mg \cdot kg^{-1}$). The nasal septum mucosa was collected, and the blood and mucus were washed with saline. These were fixed in 4% paraformaldehyde solution, dehydrated with gradient ethanol followed by HE staining. The paraffin-embedded sections were observed for histopathological changes in the nasal mucosa.

Statistical analysis

All data are presented as mean of each group ± SEM. Data were analysed by one-way analysis of variance (ANOVA) and non-parametric tests, followed by Dunn's multiple comparison or Tukey's multiple comparison test. GraphPad prism version 5.0 (GraphPad) was used for charting and statistical analysis. P-values less than 0.05 are considered statistically significant.

Results

Effect of Art-TMP combination on mortality, parasitemia, and malaria parasite morphology in C57BL/6 mice infected with PbA

C57BL/6 mice infected with PbA ECM developed neurological signs on d6 p.i. that resulted in death between d8 and 12 p.i. (Fig. 1A, B). In contrast, only approximately 30% mice died in the Art group; deaths were observed from d10 p.i.

The TMP treatment group did not improve the survival or reduce parasitemia and death occurred on d9 to 12 p.i.. Art + TMP treatment significantly improved the outcome in ECM mice; none of the mice in this group died and parasitaemia was reported only in 10.12% mice on d12 p.i. In addition, malaria parasites could still be observed in the Art group. A decrease in late trophozoites was observed in the blood smears of the Art + TMP group as compared to the blood smears of the Infected group and TMP alone treatment group on d7 p.i. (Fig. 1C).

Art-TMP combination reduces clinical symptoms of ECM

We next utilized rapid murine coma and behaviour scale (RMCBS) to assess ECM manifestations after drug therapy. We found that ECM mice developed a score less than 4 points, consistent with their symptoms of reduced exploratory behaviour, decreased reflex, self-preservation, and finally coma and epilepsy (Fig. 2A). The score in the Art-treated mice was significantly higher than that in the ECM mice in later stages of infection. Particularly, mice in the Art + TMP group presented distinctly higher RMCBS values as compared to ECM mice (Fig. 2A). Results also showed significant differences between the Art + TMP and the Art groups at 9 to 11 days p.i. The value was higher than 12 points in the Art + TMP group on d12 p.i. (Fig. 2A).

ECM mice (15.68 g) and TMP-treated mice (14.82 g) showed significantly lower weight on d7 p.i. as compared with the weight of mice in the Art (18.72 g) or Art + TMP treatment group (18.10 g), even until on d12 p.i. (Fig. 2B). The weight of mice in the Art + TMP group (18.05 g) was found to be higher than that of mice in the Art

group (17.63 g) from d8 p.i. to d12 p.i. (Fig. 2B).

There was no significant difference in the body temperature of mice between the TMP group and the Infected group. However, on d9 p.i. and d11 p.i., the body temperature of mice in the Art group (33.2°C, 33.13°C) and the Art + TMP group (35.4°C, 34.59°C) was significantly higher than that in the TMP group (30.65°C, 27.42°C) and Infected group (29.48°C, 28.85°C) ($p < 0.001$). More noteworthy was the fact that the body temperature of mice in the Art + TMP group was significantly higher than that of mice in the Art group on d9 p.i. and d11 p.i. ($p < 0.01$, $p < 0.05$) (Fig. 2C).

Art-TMP combination enhances the exploratory locomotion in ECM mice

The open field test was used to investigate the ability of autonomous activity (locomotion, exploration, and anxiety) in mice, as shown in Fig. 3A. The PbA-infected mice travelled shorter distances than control mice. Compared with the ECM mice (395.63 cm), the mice in the Art group and the Art + TMP group could travel longer distances in the open field experiment (845.82 cm for Art, 1081.59 cm for Art + TMP), which is consistent with our assessment of mice status using RMCBS. Notably, the results showed significant differences between mice in the Art and Art + TMP groups (Fig. 3A). Similarly, the total movement time that mice in the Art (75.02 s) and Art + TMP groups (82.13 s) spent was significantly longer than the time spent by mice in the Infected group (36.12 s) (Fig. 3B). Although significant differences in the distance travelled and the time spent in the central area were

observed between mice in the Art, Art + TMP and Infected groups (Fig. 3C, 3D), all mice in the four groups did not differ in the percentage of distance travelled in the centre of the open field (Fig. 3E), indicating that mice that travelled longer distances and spent more time in the central area did not show an anxiety-like state.

To study the effectiveness of new treatments on CM in animal models, animals were tested for spontaneous alternation in the Y maze. All drug-treated mice performed to similar extent in this test. The total number of times into arms (±SEM) was 16.00 times for Art, 17.62 times for TMP and 23.75 times for the Art + TMP mice. Consistent with stronger autonomous activity, Art + TMP mice spent significantly more time into the arms of the maze (23.75 times vs. 16.00 times) compared with the Art mice (Fig. 3E). It is suggested that the Art + TMP combination could increase the spontaneous alternation of mice and enhance the ability of autonomous activity and exploration to the novel environment.

Art-TMP combination reduces cerebrovascular pathology and increases vessel integrity and patency

We next checked the hypothesis that the Art-TMP combination had a more profound effect than the Art and TMP alone on brain pathology. We found significantly fewer adherent leukocytes in mice in the Art + TMP group than in the untreated mice on d7 p.i. (Fig. 4A). In addition, MRI is considered as a valuable visualisation tool for tracking microvascular pathological changes *in vivo* [24]. To investigate whether the Art-TMP combination could improve vascular damage, mice

353 in the four groups (n = 6) were measured by MRI. More abundant and unobstructed
354 blood vessels were observed in mice in the Art + TMP group as compared with the
355 dramatic reduction of vessel integrity and patency in untreated PbA-infected mice
356 (Fig. 4B), which is consistent with our pathological results using HE staining. We
357 next evaluated the changes in the expression levels of adhesion molecules in brain
358 blood vessels, and found that the expression of ICAM-1 and VCAM-1 was
359 significantly decreased in the Art + TMP group mice as compared with expression of
360 these molecules in the ECM mice (Fig. 4D, E, $p < 0.001$). There was still a significant
361 difference in the number of ICAM-1- and VCAM-1-positive vessels between mice in
362 the Art + TMP and Art alone groups (Fig. 4D, 4E, $p < 0.05$, $p < 0.01$). In summary,
363 these results showed that the overall protective effect of Art + TMP treatment was to
364 help relax and widen the blood vessels and alleviate pathological damage.
365
366 **Art-TMP combination inhibits activation of astrocytes in the cortex and**
367 **maintains neuronal vitality in hippocampus**
368 Activation of astrocytes and microglia acts as a crucial player in several
369 pathophysiological changes in the central nervous system (CNS) [25]. Glial fibrillary
370 acidic protein (GFAP) is a key protein expressed in astrocytes and is significantly
371 up-regulated when nerves are damaged [26].We assessed astrocyte activation using
372 the known astrocyte marker GFAP. The number of GFAP-positive cells in the brains
373 of mice in the Art + TMP group significantly decreased as compared with that in mice
374 in the Infected group and Art group (Fig. 5B, $p < 0.05$, $p < 0.01$).

375 Immunohistochemistry using anti-NeuN antibody was performed to assess neuronal
376 viability [27]; the number of NeuN-positive cells significantly increased in the brains
377 of mice in the Art + TMP group as compared with that in mice in the Art,
378 TMP-treated and Infected mice.

379

380 **Modulation of cytokine production by Art-TMP combination in ECM mice**

381 Cognitive deficits have been reported to be associated with changes in
382 neurotrophic factors [28], including BDNF and nerve growth factor (NGF).
383 Considering that neurological dysfunction of CM is associated with cognitive
384 impairment, we studied the changes in the concentration of neurokines in mice treated
385 with drugs. Our results showed that mice in the Art + TMP group showed
386 significantly elevated levels of BDNF and NT-3 as compared with mice in the
387 infected group (Fig. 6A, 6B, $p < 0.01$). The secretion of growth factors can promote
388 endothelial cell proliferation and neovascularisation in the perivascular region,
389 resulting in tissue repair. Our study revealed that the levels of b-NGF and VEGF-A in
390 mice in the Art + TMP group were higher than those in mice in the Infected group.
391 Interestingly, these were significantly higher than those in the Art group (Fig. 6C, 6D,
392 $p < 0.001$). In addition, levels of pro-inflammatory factor TNF-α were also
393 significantly lower in mice in the Art and Art + TMP groups than those in mice in the
394 Infected group (Fig. 6E, $p < 0.01$).

395

396 **Proteomic analysis: differentially regulated proteins among treatments**

Both Art and TMP are known to improve the neurological symptoms of ECM mice. We therefore performed a proteome analysis to obtain further information about the protein profiles in the presence of Art alone, TMP alone and Art-TMP combination. Among the four treatments, a total of 5,324 proteins were identified. We screened 192 differentially expressed proteins (DEPs) following treatment with Art; of these, 128 and 64 proteins were found to be down- and up-regulated, respectively. There were 41 up-regulated DEPs and 48 down-regulated DEPs in the TMP group and 177 up-regulated and 217 down-regulated proteins in the Art + TMP group versus the ECM group. A total of 142 and 99 proteins were found to be up- and down-regulated in the Art + TMP group and the Art group, respectively. The Art + TMP versus the TMP group included 133 up-regulated and 107 down-regulated DEPs. These DEPs comprised 12 and 16 up- and down-regulated proteins, respectively, overlapping among treatments. Detailed information can be found in the S1 Table and S2 Table. The top 10 most significant brain DEPs in the Art, TMP and Art + TMP groups can be found in the S3 Table . We then compared the brain proteins that increased in mice in Art, TMP, and Art + TMP groups relative to those in the Infected mice. As illustrated by the Venn diagram in Fig. 7A, a set of 12 proteins (ANR63, NRP2, RGS9, PENK, PLD2, BMP1, LIGO2, EPHA5, CC85B, NCKX4, CHAP1, and NASP) were elevated in all drug groups. As shown in Fig. 7B, levels of a set of 16 proteins (MYL1, NFL, PERI, NFH, LPAR1, H32, K22E, MYH4, K1C15, ARMD3, PCP, K2C79, RFA3, MTNA, PP4P2, and S22A4) were found to be reduced in all drug groups. Proteins unique to the Art + TMP group included those

419 belonging to the neuroprotective pathway (SEMCB1, HAX1, CD5R1, HPCA,
420 GARE1, CD166, PC4L1, TIAM2, ROBO2, and SLIT2) and cerebrovascular
421 protection pathway (BAIP3 and PCP4L1).
422
423 **Functional enrichment analysis**
424 We observed more up- and down-regulated proteins in the Art-TMP combination
425 treated mice than in mice treated with either Art or TMP individually, which is
426 consistent with improved effects exerted by Art-TMP combination administration
427 than Art or TMP treatment alone in ECM mice. Therefore, we focused on DEPs
428 specific to the Art-TMP combination group to perform GO and KEGG enrichment
429 analyses to obtain more information about the mode of action of the combination
430 therapy. GO term enrichment revealed that most DEPs were involved in protein
431 activation cascades, B cell-mediated immunity and its regulation,
432 immunoglobulin-mediated immune response and its regulation, humoral immune
433 response and positive regulation of immunoglobulins. Detailed information is
434 provided in Fig. 7C. Notably, functions of DEPs in the Art, TMP, and Art-TMP
435 combination groups mainly involved binding, catalytic activity, regulation of
436 molecular functions, transporter activity, and structural molecules activity; these are
437 majorly involved in cellular processes, biological regulation, metabolic processes, and
438 response to stimuli. We annotated all identified DEPs of Art, TMP, and Art-TMP
439 combination groups using the KEGG database and mapped these to 166, 72, and 234
440 KEGG pathways, respectively. 8, 3 and 20 pathways in Art, TMP, and Art-TMP

441 combination treatment groups were considered statistically significant, respectively,
442 including those involved in systemic lupus erythematosus, protein digestion and
443 absorption, complement and coagulation cascades, glycerophospholipid metabolism,
444 neuroactive ligand–receptor interaction, nitrogen metabolism, haematopoietic cell
445 lineage, and *Staphylococcus aureus* infection in the Art group (Fig. 7D-Art);
446 nucleotide excision repair, phototransduction, and Fanconi anaemia pathway in the
447 TMP group (Fig. 7D-TMP); complement and coagulation cascades, thyroid hormone
448 synthesis, mismatch repair, *S. aureus* infection, systemic lupus erythematosus,
449 glycosaminoglycan biosynthesis-heparan sulfate/heparin, glucagon signalling
450 pathway, cortisol synthesis and secretion, nitrogen metabolism, cocaine addiction,
451 renin secretion, Fanconi anaemia pathway, alcoholism, pancreatic secretion, malaria,
452 gap junction, African trypanosomiasis, platelet activation, mineral absorption and
453 ovarian steroidogenesis in the Art-TMP combination group (Fig. 7D-Art+TMP).
454 Thus, there are more KEGG pathways involved in the Art-TMP combination
455 treatment group than in the Art or TMP treatment groups, similar to the results
456 obtained for DEPs and GO enrichment analysis in the three drug groups. We
457 speculate that the Art-TMP combination treatment may improve the neurological
458 symptoms in CM mice by interfering with the neuroactive ligand–receptor
459 interactions, transporters, and certain metabolic pathways. Of particular interest are
460 the DEPs, GO, and KEGG analyses that revealed more significant changes in the
461 Art-TMP combination treatment group than in the Art and TMP treatment groups.
462 With these results, we next focused on analysing DEPs only in the Art-TMP

463 combination treatment groups, attempting to find the mechanisms that could explain
464 the improvement of symptoms observed in ECM mice after Art-TMP combination
465 treatment.

466 To better explore the functional relationships among DEPs, a network was
467 constituted using protein–protein interactions of the significantly up-regulated and
468 down-regulated proteins in the Art-TMP combination group, as shown in Fig. 7E and
469 7F, respectively. A group of significantly up-regulated proteins was found to actively
470 interact; this included proteins involved in protein phosphorylation: Prkaca, Rab8a,
471 Adcy5, prkag2, Rps6ka2, Rap2b, and Ppp3cc, and proteins involved in the axon
472 development: Slit2, Robo2, and Cdh4. A group of significantly down-regulated
473 proteins was also found to actively interact and included proteins involved in the
474 transportation between blood and brain: Fgg, Apoh, ltih4, Hrg, Fga, Fgb, Orm1, Fn1,
475 Serpina3k, alb, Apoa1, Hpx, serpina1b, Mug1, and Fetub. Based on these findings, we
476 predicted that these different proteins may be involved in improving neurological
477 symptoms of CM in mice, thereby acting as novel candidates for Art-TMP
478 combination treated ECM mice.

479

480 **WB validation of iTRAQ analysis**

481 To verify the accuracy of the data, the selected differential proteins were
482 validated at the protein level by western blotting (WB) (Fig. 7G). Considering the
483 neuroprotective effects of Art and TMP on CM, we studied the levels of proteins that
484 demonstrated significant cardiovascular protection and neuroprotection of the brain

485 tissue proteome in the presence of drugs.

486 We selected five proteins including three up-regulated and two down-regulated
487 proteins in the Art+TMP group to validate Syntenin, Slit2, Tiam2, Emopexin and Npg
488 proteins, based on their statistical significance and biological relevance with respect to
489 improvement seen in CM. When measured by WB or WES, the significance of
490 Syntenin, Slit2 and Tiam2 proteins was validated on an independent set of brain
491 samples. Increased levels of Syntenin, Slit2 and Tiam2 proteins in Art, TMP and
492 Art+TMP groups were significantly higher than those in the Infected group. The
493 levels of hemopexin and Npg proteins were significantly lower in Art, TMP and
494 Art+TMP groups as compared to their levels in the Infected group, which were
495 consistent with the iTRAQ analysis.

496

497 **Intranasal administration of artesunate combination does not affect olfactory**
498 **bulb tissue**

499 Intranasal administration of healthy C57BL/6J mice with Art-TMP combination
500 (20 $mg \cdot kg^{-1}$) or placebo solution did not result in local irritation symptoms (such as
501 asthma, cough, vomiting, asphyxia, etc.). Also no abnormalities (such as breathing,
502 exercise and behaviour) were observed in animals. The safety of administration was
503 evaluated by HE-stained histopathological sections of the olfactory bulb tissue.
504 Compared with placebo-treated mice, the treated mice did not show severe nasal
505 lesions, with only partial vasoconstriction in the connective tissue of the mucosa and
506 slight lymphocyte accumulation in the lumen. However, this pathological change also

existed in placebo-treated mice, indicating that it was unrelated to intranasal administration of Art-TMP combination.

Discussion

Cerebral malaria is the most virulent and deadliest clinical manifestation of malaria. In the Sub-Saharan Africa, five-year-old or younger children are the most susceptible to developing CM; the infection is associated with 90% mortality in this region [29]. Tragically, one in four children who recovers from CM suffers from neurological deficits, including hemiplegia, cerebellar ataxia, hypotonia, paralysis, aphasia, behavioural disorders and attention deficit [6, 30-33], indicating that elimination of the parasite does not completely improves the clinical outcomes of the infection. Thus, developing a safe, effective, and novel adjunctive therapy is the need of the hour to counter the disease.

Pathophysiology of CM is still controversial. Sequestration of pRBCs and immune cells into the brain vasculature leads to vascular obstruction, hypoperfusion and hypo-oxygenation that are considered to be the major contributors to CM. Clinical evidence from patients with CM suggests fibrinogen levels to be elevated in the brain parenchyma near cerebral blood vessels that are filled with pRBCs along with axonal injury associated with haemorrhage and demyelination [29, 34, 35]. Another clinical study on CM treatment in Cambodia reported that RBCs infected with trophozoites accumulated in the blood vessels of patients resulting in ischaemia and hypoxia in the brain, consequently causing irreversible neurological damage. Even if the patients

529 were administered artemisinin and heparin, tiny blood vessel obstructions
530 remained[36]. Therefore, it is essential to explore a method of timely clearance of the
531 microvascular occlusion to alleviate and eliminate cerebral ischaemia and hypoxia
532 injury in patients with CM and improve long-term neurological deficits and
533 dysfunction. In the present study, we used an ECM mouse model to investigate the
534 potential of TMP as an adjunctive therapy to improve the neurological symptoms and
535 survival. Results of our study revealed lower parasitaemia, better clinical outcomes,
536 improvement of histological and immunological features in ECM mice after treatment
537 with TMP + Art as compared with ECM mice. Subsequently, we performed
538 quantitative proteomic analysis to compare the brain proteome profiles of ECM mice
539 treated with Art, TMP and Art + TMP to explore the possible targets of Art + TMP in
540 treating ECM.

541 Firstly, we successfully replicated the ECM model that exhibited neurological
542 damage including hemi- and paraplegia, ataxia, and convulsions, consistent with
543 previous studies [37, 38]. ECM mice were treated by intranasal administration with
544 Art and TMP at d2 to d5 p.i. to investigate the effect of Art-TMP combination in
545 preventing the incidence of ECM at an early stage of malaria infection. Several
546 researchers have initiated empiric novel treatments of ECM administered before, on,
547 or just after the first day of infection for evaluating various effects at different stages
548 of malaria infection [39-43]. Our future studies aim to study the drug effect after 3 to
549 7 days of infection on long-term prevention of neurological damage in ECM mice. In
550 the present study, we did not observe any significant changes in parasitaemia, body

551 weight and survival status of ECM mice after TMP treatment alone. However, we
552 observed a considerable delay in death from ECM after TMP treatment from d8 p.i. to
553 d9 p.i. Moreover, mice in the Art and Art-TMP combination groups exhibited
554 prolonged survival (even close to 100%) in the Art-TMP combination group, as well
555 as a decrease in parasitaemia, and an increase in body weight and temperature. More
556 importantly, a significant decrease in the proportion of large trophozoite stage of
557 *Plasmodium* in the blood smear of the two groups was observed. Notably, a lower
558 parasitaemia and increased body weight and temperature were observed upon
559 treatment of infected mice with Art-TMP combination than those treated with Art
560 alone, suggesting that the Art-TMP combination treatment could successfully reduce
561 the pathological outcomes and improve the clinical signs in ECM mice.

562 One of our previous study has confirmed that the Art-TMP combination treatment
563 significantly improved the cerebral vascular occlusion in ECM mice than in mice in
564 the Art-treated group [44]. Same results were also observed in the present study,
565 especially the significant improvement of symptoms including decreased adhesion of
566 parasite-infected erythrocytes and immune cells to cerebral microvessels after TMP
567 monotherapy, which had the same effect as the Art-TMP combination treatment.
568 Indeed, abnormal microvascular integrity and cerebral perfusion were observed by
569 MRI in ECM mice, consistent with the findings of occlusion effect of brain
570 microvasculature in ECM mice from HE studies. We observed that Art and TMP
571 monotherapy could improve the above-mentioned symptoms, with the Art-TMP
572 combination therapy showing the most significant improvement by MRI. Activation

573 of endothelial cells is manifested in several ways, for example increased expression of
574 adhesion molecules. ICAM-1 (CD54) and CD36 are two major binding partners for
575 the PfEMP1 protein on PfRBCs that contribute to PfRBC sequestration. The
576 important factor of ICAM-1 expression in the development of CM is well established.
577 Tripathi *et al.* found that exposure of the human brain microvascular ECs to PfRBCs
578 induced the expression of ICAM-1 [45]. Favre *et al.* reported that ICAM-1-deficient
579 mice were protected from CM [46]. Interestingly, our study found that TMP
580 monotherapy and Art-TMP combination therapy significantly reduced the activation
581 of brain microvascular endothelial cells with a lower expression of ICAM-1 and
582 VCAM-1 in the endothelial cells of ECM mice than that in the untreated ECM model
583 mice. However, no significant effect of Art monotherapy on endothelial activation
584 among ECM mice was observed. These results demonstrate that Art-TMP
585 combination plays a major role in defining the pathological outcomes and clinical
586 signs in ECM mice. Specifically, Art exerts a direct killing effect on *Plasmodium*
587 parasite. TMP may play roles in decreasing endothelial activation, reducing
588 sequestration of iRBC and adhesion of leukocytes, and increasing blood perfusion in
589 the brain, whereas a combination of the two drugs exerts a potent synergistic effect on
590 mouse survival, parasitemia, and body weight and temperature.

591 RMCBS can evaluate the related behavior of mice to reflect the real-time
592 function of central nervous system, it can be used to objectively evaluate the disease
593 process of mice and provide a tool for evaluating new adjuvant therapies. During the
594 observation period, ECM mice gradually showed signs of walking instability, ataxia,

595 fur curl, arch back, decreased toe response and disappearance of auricle reflex,
596 convulsions, coma symptoms and death. The results of RMCBS score were consistent
597 with those of mice. In this study, significant improvement in the RMCBS scores of
598 ECM mice was observed in Art-treated group. Moreover, the Art-TMP combination
599 also significantly improved the RMCBS scores of mice at d9, 10, 11 p.i. as compared
600 with the Art group, suggesting that Art-TMP combination exerted synergistic effects
601 on improving coordination, exploration, muscle strength, reflex, self-protection and
602 health behaviour of ECM mice. Based on the ECM-specific neurological and
603 behavioural evaluation, we confirmed that the combination of Art and TMP prevented
604 significant deterioration of neurological functions. Furthermore, we evaluated whether
605 this combination could improve cognitive and behavioural changes in ECM mice, and
606 further investigated the effects on long-term neurological dysfunction in CM.

607 The open field test can qualitatively and quantitatively monitor the spontaneous
608 activity of experimental animals. Our results showed that the Art alone and the Art
609 -TMP combination changed the total moving distance and total movement time of
610 ECM mice, which is in agreement with the results of RMCBS score, suggesting that
611 the Art therapy and Art-TMP combination have a definite impact on the athletic
612 ability and exploring behaviour of ECM mice. The results of the Y maze test also
613 indicated that the Art group and Art + TMP combined group significantly affected the
614 total number of arms and improved the behaviour function to a certain extent,
615 suggesting that the adjunctive therapy could protect against ECM-induced behaviour
616 impairment.

617 Notably, previous studies have implicated anxiety-like behaviour to occur in ECM
618 mice in the open field experiment[31]. However, in our ECM model, we did not
619 observe any increase in the activity of mice in the central area of the empty field and
620 other anxious activities. We did observe a significant difference in the activity of the
621 central area of the empty field. A possible explanation for this could be that the ECM
622 mice model established in our laboratory mainly exhibited degenerative changes in
623 spontaneous activity and exploring behaviour, thus showing contracture, apathetic,
624 reduced activity, reduced response to the stimulus, and gradually appeared chest,
625 hemiplegia and convulsions symptoms. The overall state of our mice was different
626 from the anxiety-like changes reported in the literature; however, a combination of the
627 Art + TMP revered these effects in different regions of the empty field. The TMP
628 (alone) administration had no significant impact on the relevant indicators of exercise,
629 exploration, and cognition.

630 We next confirmed the synergistic effect of the Art-TMP combination treatment
631 on neurobehavioural signs in ECM mice with a further exploration of the
632 neuroprotective efficacy in ECM mice. Astrocytes are common CNS-residing cells
633 that are essential for regulating the blood flow and maintaining the blood–brain
634 barrier, thus maintaining the immune defences in the CNS. Alteration of the cerebral
635 microcirculation is an important factor in the pathogenesis of CM. Sequestered
636 PfRBCs interact closely with the cerebrovasculature, enhancing permeability,
637 endothelial activation, and vascular obstruction, thereby contributing to cerebral
638 microcirculatory alterations. As shown by our HE staining results, large trophozoite

639 parasite pRBCs and WBCs adhered to the brain microvessels of ECM mice, leading
640 to ischaemia and hypoxic injury. Trophozoite-mediated occlusion of microvessels
641 also activated the glial cells (Figs. 4 and 5). After drug administration, the number of
642 GFAP-positive cells in the cerebral cortex of mice in the Art-TMP combination group
643 significantly reduced. Moreover, the abnormal activation of astrocytes was decreased.
644 The Art-TMP combination administration also enhanced the expression of neuronal
645 NeuN in the hippocampus, suggesting the neuroprotective effects of this combination
646 against neuronal damage in ECM mice. TMP and Art-TMP combination groups could
647 significantly increase the expression levels of BDNF, NT-3 and bNGF in the brain
648 tissue, indicating the neuroprotective effect to be related to the increasing supply of
649 neurotrophins and enhanced neuronal repair and regeneration. Both single TMP
650 administration and Art-TMP combination elevated the expression of VEGF-A,
651 suggesting that TMP treatment could promote the proliferation of endothelial cells
652 and the formation of new blood vessels surrounding the site of injury, thus restoring
653 the blood supply to the ischaemic tissue and diminishing the harmful effects of
654 ischaemia on the brain tissue. Interestingly, single Art treatment had no significant
655 effect on the above signs, suggesting its inability to relieve the complications of nerve
656 damage caused by microvascular occlusion in ECM mice even after killing of the
657 *Plasmodium* parasite. However, the TMP treatment of ECM mice improved the above
658 conditions via improving the nerve nutritional status, promoting neuronal and vascular
659 tissue repair and regeneration, and other ways of restoring damaged neurological
660 function in ECM mice. Given that Art alone was unable to improve the neurological

661 protective function, the effect of single TMP on the complication of ECM above was
662 consistent with the Art-TMP combination therapy with equal effectiveness. We
663 speculate that the protective effect of Art-TMP combination therapy against
664 neurological functional deterioration could be a major effect of TMP.

665 A synergistic intervention between Art and TMP reflects 'division of labour' in
666 ECM mice. We used proteomics and bioinformatics to identify the potential
667 synergistic mechanism of these two drugs. The present study identified the DEPs
668 profiles before and after pharmacological treatments in ECM brain samples, followed
669 by enrichment analysis and network analysis to discover the changes in proteins in
670 response to drug administration. These analyses provided vital clues with respect to
671 the mechanism of action of drug or biomarkers and toxicity that could guide future
672 clinical trials. A total of 28 DEPs were identified to be significantly differentially
673 expressed among the Art, TMP and Art-TMP combination groups. Our study found
674 that there were more up- and down-regulated proteins in the Art-TMP combination
675 treated mice than in mice treated with either of the individual drugs Art and TMP, a
676 finding consistent with the therapeutic improved effects of the Art-TMP combination
677 administration as compared to Art alone and TMP alone treatments in ECM mice.
678 Therefore, we focused on studying DEPs specific to Art-TMP combination
679 administration and performed GO and KEGG enrichment analyses. GO analysis
680 revealed these DEPs to be associated with immune response and receptor regulator
681 activity, whereas the KEGG analysis found these to be associated with platelet
682 activation, African trypanosomiasis, malaria, nitrogen metabolism, systemic lupus

683 erythematosus, and complement and coagulation cascades. The PPI network analysis
684 of up- and down-regulated proteins of the Art-TMP combination group revealed
685 differentially up-regulated proteins to be related to axon development. This included
686 PRKACA protein that has been reported to be down-regulated and may be involved in
687 the neuronal damage in patients with Parkinson's disease [47]. However, our study
688 found the PRKACA-centred protein pathway to be up-regulated in ECM mice after
689 Art-TMP combination therapy, demonstrating this pathway to be involved in the
690 molecular mechanism of action of drugs. Similarly, the PPI analysis revealed the
691 down-regulated proteins specific to the Art-TMP combination group to be centred on
692 the blood–brain transport, which plays important roles in the pathological
693 improvement of ECM. Together, the bioinformatics studies predicted that the
694 neuroprotective effects of the combined Art and TMP therapy may be associated with
695 axon development or blood–brain transport.

696 We identified two down-regulated proteins, hemopexin and Ngp and three
697 up-regulated proteins, namely Slit2, Tiam2 and Syntenin in the ECM mice brain
698 tissues treated with drugs. Our WB validation analyses showed that the protein levels
699 of Slit2, Tiam2, Syntenin, Hemopexin, and Ngp matched with the changes in the
700 levels of proteins in the ECM mice by iTRAQ analysis after combined Art and TMP
701 treatment. Up-regulation of hemopexin has been reported in the PbA-infected brain
702 tissues as compared to the Pb NK65 (a *Plasmodium* strain that do cause ECM) and
703 control mice [48]. Our research revealed reduced levels of hemopexin in ECM mice
704 by the iTRAQ analysis, especially in the Art-TMP combination treated group by WB

705 validation. These findings indicated that this protein may be involved in the ECM
706 pathogenesis, and Art and TMP administration reversed pathological functions of
707 hemopexin leading to a reversal of pathogenic neurological signs and enhancing the
708 viability of neuronal cells in ECM mice.

709 We identified elevated levels of various complement components, immunoglobulin
710 components, and factors involved in the coagulation cascade in ECM mice.
711 Dysregulation of the coagulation system is a characteristic feature of severe malaria
712 and impaired synthesis of clotting factors is a pathological reason behind it. Syntenin
713 is one of the intracellular adaptor proteins that interacts with several proteins and
714 regulates a number of pathways, such as immune-related pathways and those
715 regulating angiogenesis and axonal growth [49, 50]. In our study, Syntenin was found
716 to be elevated in ECM mice treated with Art-TMP combination, suggesting that
717 complement and coagulation cascade pathways may be altered significantly as a
718 consequence of up-regulation of the immune-associated proteins, such as Syntenin.
719 This may also explain why neurological signs improved in the Art- and TMP-treated
720 ECM mice. In addition to immune-related pathways, Slit–Robo signalling pathway
721 also governs axon growth and angiogenesis. Interestingly, Slit2 protein was also
722 up-regulated in the ECM mice brain after administration of Art and TMP, providing
723 further evidence for the mechanism of action of these drugs that involves axon growth
724 and angiogenesis.

725 Intranasal administration offers several advantages including high bioavailability,
726 no liver first-pass effect, rapid absorption, and rapid onset of action of drugs that can

727 easily enter the cerebrospinal fluid in the CNS, thus specifically targeting the brain. In
728 ECM mice, a previous study reported the intranasal delivery of the anti-malarial drug
729 Art to be an efficient way to contribute to decreasing malaria-related mortality [51].
730 Similarly, we treated ECM mice using Art or TMP or Art-TMP combination
731 intranasally and observed the same results as reported by the above study; however,
732 we also observed TMP to play a neuroprotective role in the ECM mice as a result of
733 the targeted delivery to the brain.

734 **Conclusion**

735 In summary, we have proposed an efficient combination treatment for CM
736 employing Art and TMP, hopefully providing a potential effective adjuvant treatment
737 for the clinic. Our study demonstrated the synergistic effect of Art-TMP combination
738 treatment on ECM as compared to Art or TMP treatment alone. This protective effect
739 is consistent with the roles of the two drugs in protecting the neuronal system and
740 maintaining cerebrovascular integrity. The combination of Art and TMP increased the
741 survival of ECM mice, prevented damage to the nervous system and improved clinical
742 outcomes. These effects were associated with decreased cerebrovascular occlusion,
743 increased expression of neurotrophic factors, increased blood flow to the damaged
744 area, decreased expression of ICAM-1 and VCAM-1 in the brain endothelium, better
745 integrity of the cerebrovasculature and reduced inflammatory factors in the ECM mice
746 brain. These results indicated that Art-TMP combination could act as an effective
747 therapy for CM with neuroprotective, anti-inflammatory and cerebrovascular integrity
748 preservation effects. Despite the positive synergistic effects of the combination of Art

749 and TMP, one caveat of our research is the use of a low dose of Art, which could only
750 decreased the parasitaemia in the ECM mouse model. Further studies using curative
751 doses of Art combined with TMP are warranted to mimic the situations in human CM.
752 Considering the short-term therapy of TMP to be safe, clinical trials on TMP will help
753 determine its potential as an adjunct treatment for human CM. To study the possible
754 targets of Art-TMP combination in treating ECM, iTRAQ proteomics was performed
755 that revealed 217 down-regulated and 177 up-regulated proteins in the combined Art
756 and TMP group, indicating a significantly altered proteome profile as compared to
757 that of the Art or TMP alone group. Functional enrichment analysis revealed the
758 pharmacological effects of the combination of Art and TMP in the ECM mice brain
759 proteome, such as axon growth, angiogenesis, and blood–brain transport. To the best
760 of our knowledge, present study is the first comprehensive study to describe the brain
761 proteomic alterations in ECM mice treated with Art, TMP and Art-TMP combination.
762 This proteomic study not only provides the basis for further studies on mechanism of
763 action of drugs, but also assists in identifying potential biomarkers for monitoring
764 disease improvement of *Plasmodium* infection. At the same time, it enhances our
765 understanding of the pathogenesis and host responses of this fatal parasitic disease.
766 Further analysis involving patients after Art-TMP combination therapeutic
767 interventions are required to provide additional insights into the correlation of the
768 identified markers with the disease progression and their efficacy as disease
769 monitoring or prognostic indicators, which could be an informative source for future
770 persistence of the present investigation.

Abbreviations

CM: cerebral malaria; Art: artesunate; TMP: Tetramethylpyrazine; pRBC: parasitized red blood cells ; ECM: experimental cerebral malaria; SR: survival rate; RMCBS: rapid murine coma and behaviour scale; ICAM-1: intercellular adhesion molecule-1; VCAM-1: vascular cell adhesion molecule-1; GFAP: glial fibrillary acidic protein; NeuN: neuron-specific nuclear protein; BDNF: brain-derived neurotrophic factor; NT-3: neurotrophic factor-3; TNF-α: tumor necrosis factor; iTRAQ: isobaric tags for relative and absolute quantification; b-NGF: b-nerve growth factor; VEGF-A: vascular endothelial growth factor A;

Acknowledgement

No applicable

Funding

This research is supported by the Fundamental Research Funds for the Central public welfare research institutes 2017 ZZ10-024, ZXKT17001; Major National Science and Technology Program of China for Innovative Drug 2017ZX09101002-001-001-3; Exploratory Study on Deepening Antimalarial Mechanisms and Drug Resistance Mechanisms of Artemisinin 81841001; National Natural Science Foundation of China 81803814.

Availability of data and materials

The datasets during and/or analysed during the current study available from the corresponding author on reasonable request.

Authors' contributions

YL, LC and XJ designed the research. XJ, LC, ZZ, YG, KL, TY, SQ and HL carried out experiments. XZ, LC, YC and XW provided guidance and access to materials and resources. YL,

XJ and LC performed the analysis. YL, XJ and LC wrote the manuscript. All authors read and approved the final manuscript.

Consent for publication

Not applicable.

Competing interests statement

The authors declare that they have no competing interests.

Author details

Artemisinin Research Center China Academy of Chinese Medical Sciences.

References

1. Organization WH. World malaria report 2018. 2018.

2. Idro R, Carter JA, Fegan G, Neville BG, Newton CR. Risk factors for persisting neurological and cognitive impairments following cerebral malaria. Archives of disease in childhood. 2006;91(2):142-8. doi: 10.1136/adc.2005.077784. PubMed PMID: 16326798; PubMed Central PMCID: PMC2082712.

3. Reyburn H. New WHO guidelines for the treatment of malaria. Bmj. 2010;340:c2637. doi: 10.1136/bmj.c2637. PubMed PMID: 20511305.

4. Klionsky DJ, Abdelmohsen K, Abe A, Abedin MJ, Abeliovich H, Acevedo Arozena A, et al. Guidelines for the use and interpretation of assays for monitoring autophagy (3rd edition). Autophagy. 2016;12(1):1-222. doi: 10.1080/15548627.2015.1100356. PubMed PMID: 26799652; PubMed Central PMCID: PMC4835977.

5. John CC, Bangirana P, Byarugaba J, Opoka RO, Idro R, Jurek AM, et al. Cerebral

815 malaria in children is associated with long-term cognitive impairment. Pediatrics.
816 2008;122(1):e92-9. doi: 10.1542/peds.2007-3709. PubMed PMID: 18541616; PubMed
817 Central PMCID: PMC2607241.
818 6. Idro R, Kakooza-Mwesige A, Asea B, Ssebyala K, Bangirana P, Opoka RO, et al.
819 Cerebral malaria is associated with long-term mental health disorders: a cross sectional
820 survey of a long-term cohort. Malaria journal. 2016;15:184. doi: 10.1186/s12936-016-1233-6.
821 PubMed PMID: 27030124; PubMed Central PMCID: PMC4815157.
822 7. van der Heyde HC, Nolan J, Combes V, Gramaglia I, Grau GE. A unified hypothesis for
823 the genesis of cerebral malaria: sequestration, inflammation and hemostasis leading to
824 microcirculatory dysfunction. Trends in parasitology. 2006;22(11):503-8. doi:
825 10.1016/j.pt.2006.09.002. PubMed PMID: 16979941.
826 8. Good MF, Doolan DL. Immune effector mechanisms in malaria. Current opinion in
827 immunology. 1999;11(4):412-9. doi: 10.1016/S0952-7915(99)80069-7. PubMed PMID:
828 10448141.
829 9. Sun K, Fan J, Han J. Ameliorating effects of traditional Chinese medicine preparation,
830 Chinese materia medica and active compounds on ischemia/reperfusion-induced cerebral
831 microcirculatory disturbances and neuron damage. Acta pharmaceutica Sinica B.
832 2015;5(1):8-24. doi: 10.1016/j.apsb.2014.11.002. PubMed PMID: 26579420; PubMed Central
833 PMCID: PMC4629119.
834 10. Danduga R, Dondapati SR, Kola PK, Grace L, Tadigiri RVB, Kanakaraju VK.
835 Neuroprotective activity of tetramethylpyrazine against 3-nitropropionic acid induced
836 Huntington's disease-like symptoms in rats. Biomedicine & pharmacotherapy = Biomedecine

837 & pharmacotherapie. 2018;105:1254-68. doi: 10.1016/j.biopha.2018.06.079. PubMed PMID:
838 30021362.
839 11. Lu F, Li X, Li W, Wei K, Yao Y, Zhang Q, et al. Tetramethylpyrazine reverses
840 intracerebroventricular streptozotocin-induced memory deficits by inhibiting GSK-3beta. Acta
841 biochimica et biophysica Sinica. 2017;49(8):722-8. doi: 10.1093/abbs/gmx059. PubMed
842 PMID: 28633346.
843 12. Wu W, Yu X, Luo XP, Yang SH, Zheng D. Tetramethylpyrazine protects against
844 scopolamine-induced memory impairments in rats by reversing the cAMP/PKA/CREB
845 pathway. Behavioural brain research. 2013;253:212-6. doi: 10.1016/j.bbr.2013.07.052.
846 PubMed PMID: 23916742.
847 13. Mohanty S, Patel DK, Pati SS, Mishra SK. Adjuvant therapy in cerebral malaria. The
848 Indian journal of medical research. 2006;124(3):245-60. PubMed PMID: 17085828.
849 14. Varo R, Crowley VM, Sitoe A, Madrid L, Serghides L, Kain KC, et al. Adjunctive therapy
850 for severe malaria: a review and critical appraisal. Malaria journal. 2018;17(1):47. doi:
851 10.1186/s12936-018-2195-7. PubMed PMID: 29361945; PubMed Central PMCID:
852 PMC5781278.
853 15. White NJ, Turner GD, Medana IM, Dondorp AM, Day NP. The murine cerebral malaria
854 phenomenon. Trends in parasitology. 2010;26(1):11-5. doi: 10.1016/j.pt.2009.10.007.
855 PubMed PMID: 19932638; PubMed Central PMCID: PMC2807032.
856 16. Riggle BA, Miller LH, Pierce SK. Do we know enough to find an adjunctive therapy for
857 cerebral malaria in African children? F1000Research. 2017;6:2039. doi:
858 10.12688/f1000research.12401.1. PubMed PMID: 29250318; PubMed Central PMCID:

PMC5701444.

17. He X, Yan J, Zhu X, Wang Q, Pang W, Qi Z, et al. Vitamin D inhibits the occurrence of experimental cerebral malaria in mice by suppressing the host inflammatory response. Journal of immunology. 2014;193(3):1314-23. doi: 10.4049/jimmunol.1400089. PubMed PMID: 24965778; PubMed Central PMCID: PMC4110641.

18. Carroll RW, Wainwright MS, Kim KY, Kidambi T, Gomez ND, Taylor T, et al. A rapid murine coma and behavior scale for quantitative assessment of murine cerebral malaria. PloS one. 2010;5(10). doi: 10.1371/journal.pone.0013124. PubMed PMID: 20957049; PubMed Central PMCID: PMC2948515.

19. Walsh RN, Cummins RA. The Open-Field Test: a critical review. Psychological bulletin. 1976;83(3):482-504. PubMed PMID: 17582919.

20. Suryavanshi PS, Ugale RR, Yilmazer-Hanke D, Stairs DJ, Dravid SM. GluN2C/GluN2D subunit-selective NMDA receptor potentiator CIQ reverses MK-801-induced impairment in prepulse inhibition and working memory in Y-maze test in mice. British journal of pharmacology. 2014;171(3):799-809. doi: 10.1111/bph.12518. PubMed PMID: 24236947; PubMed Central PMCID: PMC3969090.

21. Du Y, Chen G, Zhang X, Yu C, Cao Y, Cui L. Artesunate and erythropoietin synergistically improve the outcome of experimental cerebral malaria. International immunopharmacology. 2017;48:219-30. doi: 10.1016/j.intimp.2017.05.008. PubMed PMID: 28531845.

22. Ding WY, Li YH, Lian H, Ai XY, Zhao YL, Yang YB, et al. Sub-Minimum Inhibitory Concentrations of Rhubarb Water Extracts Inhibit Streptococcus suis Biofilm Formation.

881 Frontiers in pharmacology. 2017;8:425. doi: 10.3389/fphar.2017.00425. PubMed PMID:
882 28736523; PubMed Central PMCID: PMC5500959.
883 23. Wisniewski JR, Zougman A, Nagaraj N, Mann M. Universal sample preparation method
884 for proteome analysis. Nature methods. 2009;6(5):359-62. doi: 10.1038/nmeth.1322. PubMed
885 PMID: 19377485.
886 24. Hoffmann A, Helluy X, Fischer M, Mueller AK, Heiland S, Pham M, et al. In Vivo Tracking
887 of Edema Development and Microvascular Pathology in a Model of Experimental Cerebral
888 Malaria Using Magnetic Resonance Imaging. Journal of visualized experiments : JoVE.
889 2017;(124). doi: 10.3791/55334. PubMed PMID: 28654030; PubMed Central PMCID:
890 PMC5608346.
891 25. De Luca C, Savarese L, Colangelo AM, Bianco MR, Cirillo G, Alberghina L, et al.
892 Astrocytes and Microglia-Mediated Immune Response in Maladaptive Plasticity is Differently
893 Modulated by NGF in the Ventral Horn of the Spinal Cord Following Peripheral Nerve Injury.
894 Cellular and molecular neurobiology. 2016;36(1):37-46. doi: 10.1007/s10571-015-0218-2.
895 PubMed PMID: 26084599.
896 26. Brenner M. Role of GFAP in CNS injuries. Neuroscience letters. 2014;565:7-13. doi:
897 10.1016/j.neulet.2014.01.055. PubMed PMID: 24508671; PubMed Central PMCID:
898 PMC4049287.
899 27. Zhang T, Gu J, Wu L, Li N, Sun Y, Yu P, et al. Neuroprotective and axonal
900 outgrowth-promoting effects of tetramethylpyrazine nitrone in chronic cerebral hypoperfusion
901 rats and primary hippocampal neurons exposed to hypoxia. Neuropharmacology.
902 2017;118:137-47. doi: 10.1016/j.neuropharm.2017.03.022. PubMed PMID: 28342896.

903 28. Budni J, Bellettini-Santos T, Mina F, Garcez ML, Zugno AI. The involvement of BDNF,
904 NGF and GDNF in aging and Alzheimer's disease. Aging and disease. 2015;6(5):331-41. doi:
905 10.14336/AD.2015.0825. PubMed PMID: 26425388; PubMed Central PMCID: PMC4567216.
906 29. Dorovini-Zis K, Schmidt K, Huynh H, Fu W, Whitten RO, Milner D, et al. The
907 neuropathology of fatal cerebral malaria in malawian children. The American journal of
908 pathology. 2011;178(5):2146-58. doi: 10.1016/j.ajpath.2011.01.016. PubMed PMID:
909 21514429; PubMed Central PMCID: PMC3081150.
910 30. Guha SK, Tillu R, Sood A, Patgaonkar M, Nanavaty IN, Sengupta A, et al. Single
911 episode of mild murine malaria induces neuroinflammation, alters microglial profile, impairs
912 adult neurogenesis, and causes deficits in social and anxiety-like behavior. Brain, behavior,
913 and immunity. 2014;42:123-37. doi: 10.1016/j.bbi.2014.06.009. PubMed PMID: 24953429.
914 31. de Sousa LP, de Almeida RF, Ribeiro-Gomes FL, de Moura Carvalho LJ, TM ES, de
915 Souza DOG, et al. Long-term effect of uncomplicated Plasmodium berghei ANKA malaria on
916 memory and anxiety-like behaviour in C57BL/6 mice. Parasites & vectors. 2018;11(1):191.
917 doi: 10.1186/s13071-018-2778-8. PubMed PMID: 29554958; PubMed Central PMCID:
918 PMC5859440.
919 32. Shikani HJ, Freeman BD, Lisanti MP, Weiss LM, Tanowitz HB, Desruisseaux MS.
920 Cerebral malaria: we have come a long way. The American journal of pathology.
921 2012;181(5):1484-92. doi: 10.1016/j.ajpath.2012.08.010. PubMed PMID: 23021981; PubMed
922 Central PMCID: PMC3483536.
923 33. Shabani E, Ouma BJ, Idro R, Bangirana P, Opoka RO, Park GS, et al. Elevated
924 cerebrospinal fluid tumour necrosis factor is associated with acute and long-term

925 neurocognitive impairment in cerebral malaria. Parasite immunology. 2017;39(7). doi:
926 10.1111/pim.12438. PubMed PMID: 28453871; PubMed Central PMCID: PMC5492989.
927 34. Beare NA, Lewallen S, Taylor TE, Molyneux ME. Redefining cerebral malaria by
928 including malaria retinopathy. Future microbiology. 2011;6(3):349-55. doi: 10.2217/fmb.11.3.
929 PubMed PMID: 21449844; PubMed Central PMCID: PMC3139111.
930 35. Medana IM, Day NP, Hien TT, Mai NT, Bethell D, Phu NH, et al. Axonal injury in cerebral
931 malaria. The American journal of pathology. 2002;160(2):655-66. doi:
932 10.1016/S0002-9440(10)64885-7. PubMed PMID: 11839586; PubMed Central PMCID:
933 PMC1850649.
934 36. GuoQiao Li XG, LinChun Fu,et al. Study on the timing of antimalarial treatment for
935 cerebral malaria coma patients to improve the cure rate. Compilation of Scientific Research
936 Papers on the 10th Anniversary of the Institute of Tropical Medicine, Guangzhou University of
937 Traditional Chinese Medicine. 1999:1.
938 37. Chora AA, Fontoura P, Cunha A, Pais TF, Cardoso S, Ho PP, et al. Heme oxygenase-1
939 and carbon monoxide suppress autoimmune neuroinflammation. The Journal of clinical
940 investigation. 2007;117(2):438-47. doi: 10.1172/JCI28844. PubMed PMID: 17256058;
941 PubMed Central PMCID: PMC1770945.
942 38. Renia L, Potter SM, Mauduit M, Rosa DS, Kayibanda M, Deschemin JC, et al.
943 Pathogenic T cells in cerebral malaria. International journal for parasitology.
944 2006;36(5):547-54. doi: 10.1016/j.ijpara.2006.02.007. PubMed PMID: 16600241.
945 39. Lackner P, Part A, Burger C, Dietmann A, Broessner G, Helbok R, et al. Glatiramer
946 acetate reduces the risk for experimental cerebral malaria: a pilot study. Malaria journal.

947 2009;8:36. doi: 10.1186/1475-2875-8-36. PubMed PMID: 19250545; PubMed Central PMCID:
948 PMC2651188.
949 40. Blanco YC, Farias AS, Goelnitz U, Lopes SC, Arrais-Silva WW, Carvalho BO, et al.
950 Hyperbaric oxygen prevents early death caused by experimental cerebral malaria. PloS one.
951 2008;3(9):e3126. doi: 10.1371/journal.pone.0003126. PubMed PMID: 18769544; PubMed
952 Central PMCID: PMC2518956.
953 41. Penet MF, Abou-Hamdan M, Coltel N, Cornille E, Grau GE, de Reggi M, et al. Protection
954 against cerebral malaria by the low-molecular-weight thiol pantethine. Proceedings of the
955 National Academy of Sciences of the United States of America. 2008;105(4):1321-6. doi:
956 10.1073/pnas.0706867105. PubMed PMID: 18195363; PubMed Central PMCID:
957 PMC2234136.
958 42. Cariaco Y, Lima WR, Sousa R, Nascimento LAC, Briceno MP, Fotoran WL, et al.
959 Ethanolic extract of the fungus Trichoderma stromaticum decreases inflammation and
960 ameliorates experimental cerebral malaria in C57BL/6 mice. Scientific reports.
961 2018;8(1):1547. doi: 10.1038/s41598-018-19840-x. PubMed PMID: 29367729; PubMed
962 Central PMCID: PMC5784021.
963 43. Canavese M, Crisanti A. Vascular endothelial growth factor (VEGF) and lovastatin
964 suppress the inflammatory response to Plasmodium berghei infection and protect against
965 experimental cerebral malaria. Pathogens and global health. 2015;109(6):266-74. doi:
966 10.1179/2047773215Y.0000000021. PubMed PMID: 26392164; PubMed Central PMCID:
967 PMC4727581.
968 44. Jiang XH, Chen LN, Li K, Guo Y, Zheng ZY, Yang T, et al. [Protective effects of

969 artesunate combination on experimental cerebral malaria and nerve injury]. Zhongguo Zhong
970 yao za zhi = Zhongguo zhongyao zazhi = China journal of Chinese materia medica.
971 2018;43(15):3051-7. doi: 10.19540/j.cnki.cjcmm.20180608.002. PubMed PMID: 30200698.
972 45. Tripathi AK, Sullivan DJ, Stins MF. Plasmodium falciparum-infected erythrocytes
973 increase intercellular adhesion molecule 1 expression on brain endothelium through
974 NF-kappaB. Infection and immunity. 2006;74(6):3262-70. doi: 10.1128/IAI.01625-05. PubMed
975 PMID: 16714553; PubMed Central PMCID: PMC1479273.
976 46. Favre N, Da Laperousaz C, Ryffel B, Weiss NA, Imhof BA, Rudin W, et al. Role of
977 ICAM-1 (CD54) in the development of murine cerebral malaria. Microbes and infection.
978 1999;1(12):961-8. PubMed PMID: 10617927.
979 47. Wang J, Liu Y, Chen T. Identification of key genes and pathways in Parkinson's disease
980 through integrated analysis. Molecular medicine reports. 2017;16(4):3769-76. doi:
981 10.3892/mmr.2017.7112. PubMed PMID: 28765971; PubMed Central PMCID: PMC5646954.
982 48. Moussa E, Huang H, Ahras M, Lall A, Thezenas ML, Fischer R, et al. Proteomic profiling
983 of the brain of mice with experimental cerebral malaria. Journal of proteomics. 2018;180:61-9.
984 doi: 10.1016/j.jprot.2017.06.002. PubMed PMID: 28602553.
985 49. Tomoda T, Kim JH, Zhan C, Hatten ME. Role of Unc51.1 and its binding partners in CNS
986 axon outgrowth. Genes & development. 2004;18(5):541-58. doi: 10.1101/gad.1151204.
987 PubMed PMID: 15014045; PubMed Central PMCID: PMC374236.
988 50. Azar WJ, Azar SH, Higgins S, Hu JF, Hoffman AR, Newgreen DF, et al. IGFBP-2
989 enhances VEGF gene promoter activity and consequent promotion of angiogenesis by
990 neuroblastoma cells. Endocrinology. 2011;152(9):3332-42. doi: 10.1210/en.2011-1121.

PubMed PMID: 21750048.

51. Marijon A, Bonnot G, Fourier A, Bringer C, Lavoignat A, Gagnieu MC, et al. Efficacy of intranasal administration of artesunate in experimental cerebral malaria. Malaria journal. 2014;13:501. doi: 10.1186/1475-2875-13-501. PubMed PMID: 25516091; PubMed Central PMCID: PMC4320559.

Supporting information Legends

S1 Table. Differentially expressed proteins (DEPs) following treatment with artesunate (Art), tetramethylpyrazine (TMP), Art-TMP combination (Art+TMP).

S2 Table. Down- and up-regulated differentially expressed proteins (DEPs) in the artesunate (Art), tetramethylpyrazine (TMP) and Art-TMP combination (Art+TMP) groups.

S3 Table. The top 10 most significant brain differentially expressed proteins (DEPs) in the artesunate (Art), tetramethylpyrazine (TMP) and Art-TMP combination (Art+TMP) groups .

Figure legend

Figure 1. Effect of Art-TMP combination on mortality, parasitaemia and malaria parasite morphology in mice infected with PbA-ECM. Blood was collected from the tail of mice and stained with Giemsa for analysis of parasitaemia. Daily survival was also recorded. All ECM mice were treated with a single dose of Art at 13.00 mg·kg-1, a single dose of TMP at 10.40 mg·kg-1 and a dose of Art-TMP combination at 23.40 mg·kg-1 from d2 to d5 p.i..(A) Art-TMP combination significantly prolonged the survival of ECM mice. (B) Effect of Art and Art + TMP on parasitaemia in PbA-infected mice. (C) Giemsa-stained blood smears of PbA-infected mice on day 7 p.i. (n = 13 for each group). Data are expressed as mean ± SEM in each group. The

parasitaemia was analysed by one-way ANOVA. Statistical differences associated with the infected group were marked according to the colour of the symbol of each group. ANOVA, analysis of variance; Art, artesunate; ECM, experimental cerebral malaria; PbA, Plasmodium berghei ANKA; SEM, standard error of mean; TMP, tetramethylpyrazine.

Figure 2. Art-TMP combination treatment can provide relief from clinical symptoms in ECM mice and improve weight and body temperature of ECM mice (n = 13). The weight of each mouse was counted daily from d2 p.i., RMCBS score evaluation was performed from d3 p.i. and body temperature was measured every other day. All ECM mice were treated with drugs as described above. (A) RMCBS score, (B) body weight and (C) body temperature of each group are shown. Data are expressed as mean ± SEM in each group. Data were analysed by one-way ANOVA. Statistical differences associated with the Infected group were marked according to the colour of the symbol of each group. ANOVA, analysis of variance; Art, artesunate; ECM, experimental cerebral malaria; RMCBS, rapid murine coma and behaviour scale; SEM, standard error of mean; TMP, tetramethylpyrazine.

Figure 3. Improved autonomous activity in Art + TMP mice as measured by the open field test and Y-maze spontaneous alternation test. All PbA-infected mice with ECM were treated with drugs as described above. (A) Total distance of movement in the open field test on day 7 p.i. (B) Total time of movement in the open field test on day 7 p.i. (C) Distance travelled in the central area. (D) Time spent in movement in the central area. (E) The percentage of movement distance in the central area. (F) Effect of Art, TMP, Art-TMP combination drugs on number of entries in the

closed arms following 8 minutes of maze exploration on day 8 p.i. in the Y-maze test. Data are expressed as mean ± SEM of two independent experiments. (n = 10 in control group and n = 13 in other groups). Art, artesunate; ECM, experimental cerebral malaria; PbA, Plasmodium berghei ANKA; SEM, standard error of mean; TMP, tetramethylpyrazine.

Figure 4. The efficacy of the Art-TMP combination was checked in reducing the cerebrovascular pathology and maintaining vascular integrity and patency in ECM mice. Inhibition of inflammation in the brain of PbA-infected mice after drug treatment as described above. (A) HE staining of the brain tissue sections. Arrows show the adhesion of leukocytes and pRBC to the blood vessels. All sections were stained with H&E (magnification, ×400). (B) Representative MRI images of the brain obtained by TOF-2D-FLASH scanning. (C) Representative images of ICAM-1- and VCAM-1-positive blood vessels (ICAM-1+, VCAM-1+) obtained by immunohistochemistry of the brain slices, with the arrow pointing in the direction of the microvessel. Upper right is the enlarged image of the vessel region. (D) Random ICAM-1+ blood vessels and (E) VCAM-1+ blood vessels (n = 20). Each mouse was randomly selected from 20 fields to evaluate the number of vascular expressions of ICAM-1+ and VCAM-1+ from 6 mice per group. Scale bar: 50 μm. Data are presented as mean of each group ± SEM. Data were analysed by one-way ANOVA. ANOVA, analysis of variance; Art, artesunate; ECM, experimental cerebral malaria; HE, haematoxylin and eosin; ICAM, intercellular cell adhesion molecule; MRI, magnetic resonance imaging; PbA, Plasmodium berghei ANKA; SEM, standard error of mean; TMP, tetramethylpyrazine; TOF, time-of-flight; VCAM, vascular cell adhesion molecule.

Figure 5. The Art-TMP combination suppresses astrocytes activation and sustains neuronal viability. Immunohistochemistry using anti-GFAP and anti-NeuN antibodies was performed in the brain of ECM mice after the treatments as described above. (A) Representative images of immunostaining of GFAP in the cortex and of NeuN in the hippocampus. (B, C) Quantitative analyses of GFAP-positive cells in the cortex and NeuN-positive cells in the hippocampus. Results were calculated as ratio to the Infected group and are expressed as means ± SEM (n = 6 mice in each group). Scale bar: 100 μm. ECM, experimental cerebral malaria; GFAP, glial fibrillary acidic protein; NeuN, neuron-specific nuclear protein; SEM, standard error of mean; TMP, tetramethylpyrazine.

Figure 6. Expression levels of BDNF, NT-3, b-NGF, VEGF-A and TNF-α in the brain tissue of ECM mice after treatments as described above (n = 6 in each group). Data are expressed as mean of each group ± SEM. Data were analysed by one-way ANOVA. ANOVA, analysis of variance; BDNF, brain-derived neurotrophic factor; ECM, experimental cerebral malaria; NT-3, neurotrophic factor-3; NGF, nerve growth factor; SEM, standard error of mean; TMP, tetramethylpyrazine; TNF, tumour necrosis factor; VEGF, vascular endothelial growth factor.

Figure 7. iTRAQ proteomic analysis of brain tissues in ECM mice after different drugs treatment. (A) unique up-regulated proteins overlapping among Art, TMP and Art-TMP combination treatment relative to cerebral malaria mouse. Protein names for overlapping up-regulated proteins are shown to the right of the Venn diagram. (B) unique down-regulated proteins overlapping among Art, TMP and Art-TMP combination treatment relative to cerebral malaria mouse. Protein

1079 names for overlapping up-regulated proteins are shown to the right of the Venn diagram. (C) GO
1080 annotation of differentially regulated protein (ratio: > 1.2 or < 0.8) functions. Y-axis represented
1081 the number of identified proteins in each GO category. (D) KEGG pathway analysis. KEGG
1082 pathway enrichment analysis results for comparison Art (differentially expressed proteins in Art
1083 treatment group compared with ECM mice group), for comparison TMP (differentially expressed
1084 proteins in TMP treatment group compared with ECM mice group) and comparison Art+TMP
1085 (differentially expressed proteins in Art+TMP treatment group compared with ECM mice group)
1086 are shown. The y-axes indicates the significantly enriched KEGG pathway;The x-axes represent
1087 the number of differentially expressed proteins contained in each KEGG pathway (the P value is
1088 calculated based on Fisher's exact test). The color gradient represents the magnitude of the P value
1089 and the tab above the bar shows the enrichment factor, indicating the number of differentially
1090 expressed proteins involved in a KEGG pathway as a percentage of the number of proteins
1091 involved in the pathway in all identified proteins. (E and F) The protein-protein interaction (PPI)
1092 network of proteins in Art+TMP treated groups based on STRING analysis. A total of 127
1093 differentially up-regulated proteins and 148 differentially down-regulated proteins are shown in E
1094 and F PPI network, respectively. Strong associations are represented by thicker lines. (G)
1095 Validation of the proteomics results. Western blotting analysis of five proteins selected from the
1096 proteomics data. Art, artesunate; ECM, experimental cerebral malaria; TMP, tetramethylpyrazine.
1097
1098 Figure 8. Histopathological sections of HE staining of the nasal mucosa of healthy C57BL/6J mice
1099 treated with Art + TMP combination (20 mg·kg-1) by intranasal administration. (A) A control
1100 group received intranasal administration of placebo solution. (B) C57BL/6J mice received

intranasal administration of Art + TMP once. (C) C57BL/6J mice received intranasal administration of Art + TMP four times. Scale bar: 100 μm. Red arrows indicate inflammatory cell infiltration; leukocyte aggregation can be seen in the lumen, as shown by the yellow arrow. The epithelium of the nasal mucosa is intact and cilia on the epithelium are clearly visible, as shown by the black arrow. Art, artesunate; ECM, experimental cerebral malaria; HE, haematoxylin and eosin; TMP, tetramethylpyrazine.

Fig.1

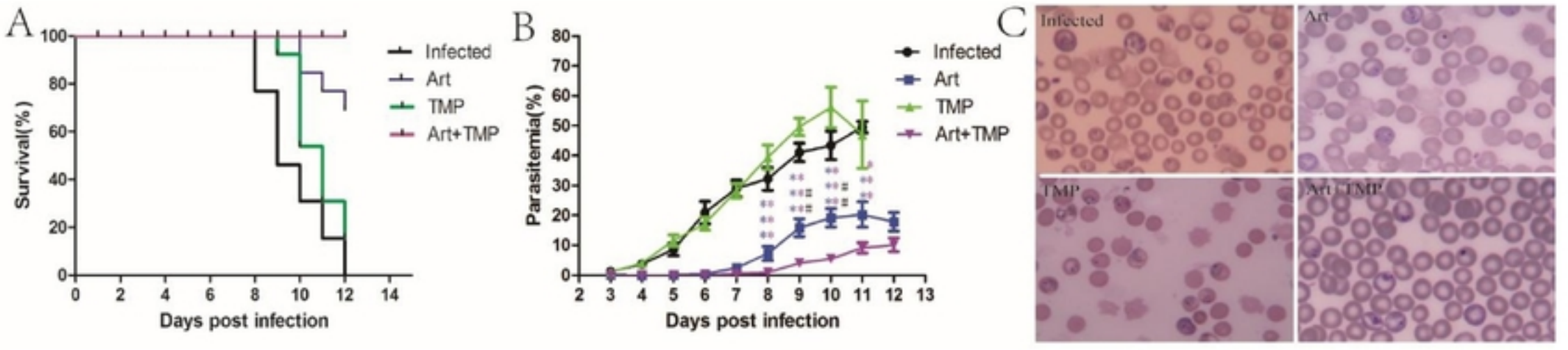
A
Survival(%)
Days post infection
Infected
Art
TMP
Art+TMP
B
Parasitemia(%)
Days post infection
Infected
Art
TMP
Art+TMP
C
Infected
Art
TMP
Art+TMP

Fig.2

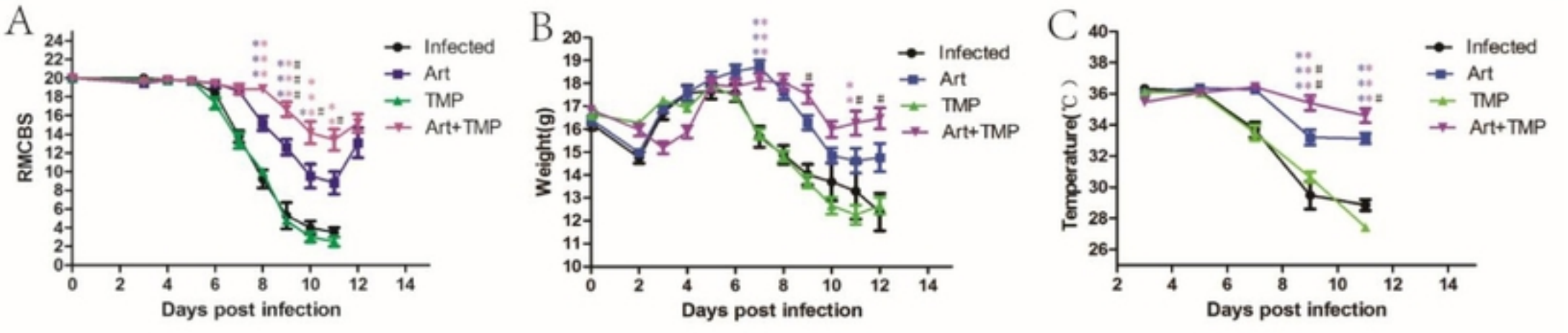
A
RMCBS
Days post infection
Infected
Art
TMP
Art+TMP
B
Weight(g)
Days post infection
Infected
Art
TMP
Art+TMP
C
Temperature(℃)
Days post infection
Infected
Art
TMP
Art+TMP

Fig.3

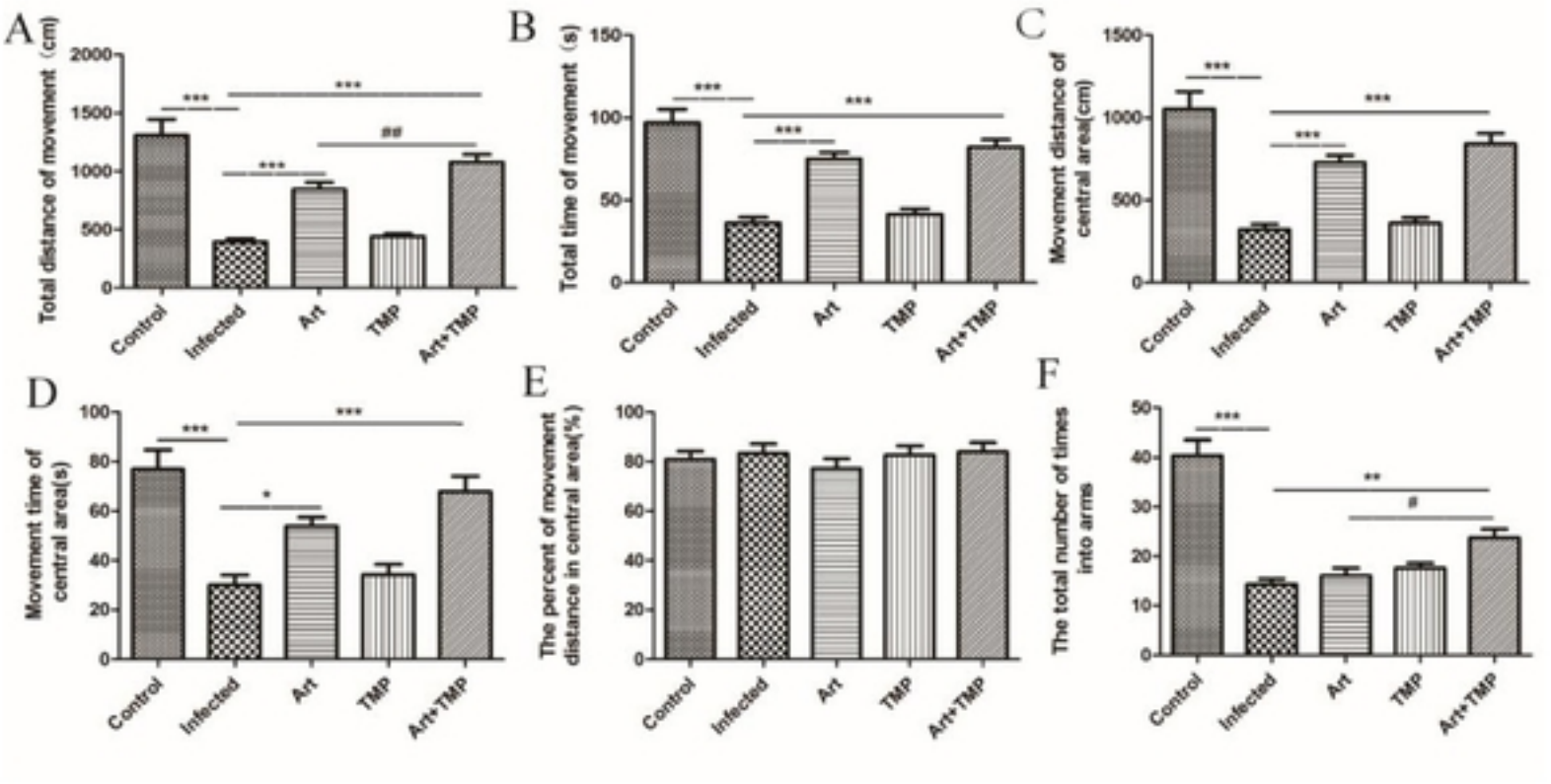
A
Total distance of movement（cm）
2000
1500
1000
500
0
***
***
***
##
Control
Infected
Art
TMP
Art+TMP
B
Total time of movement（s）
150
100
50
0
***
***
***
Control
Infected
Art
TMP
Art+TMP
C
Movement distance of central area(cm)
1500
1000
500
0
***
***
***
Control
Infected
Art
TMP
Art+TMP
D
Movement time of central area(s)
100
80
60
40
20
0
***
*
***
Control
Infected
Art
TMP
Art+TMP
E
The percent of movement distance in central area(%)
100
80
60
40
20
0
Control
Infected
Art
TMP
Art+TMP
F
The total number of times into arms
50
40
30
20
10
0
***
**
#
Control
Infected
Art
TMP
Art+TMP

Fig.4

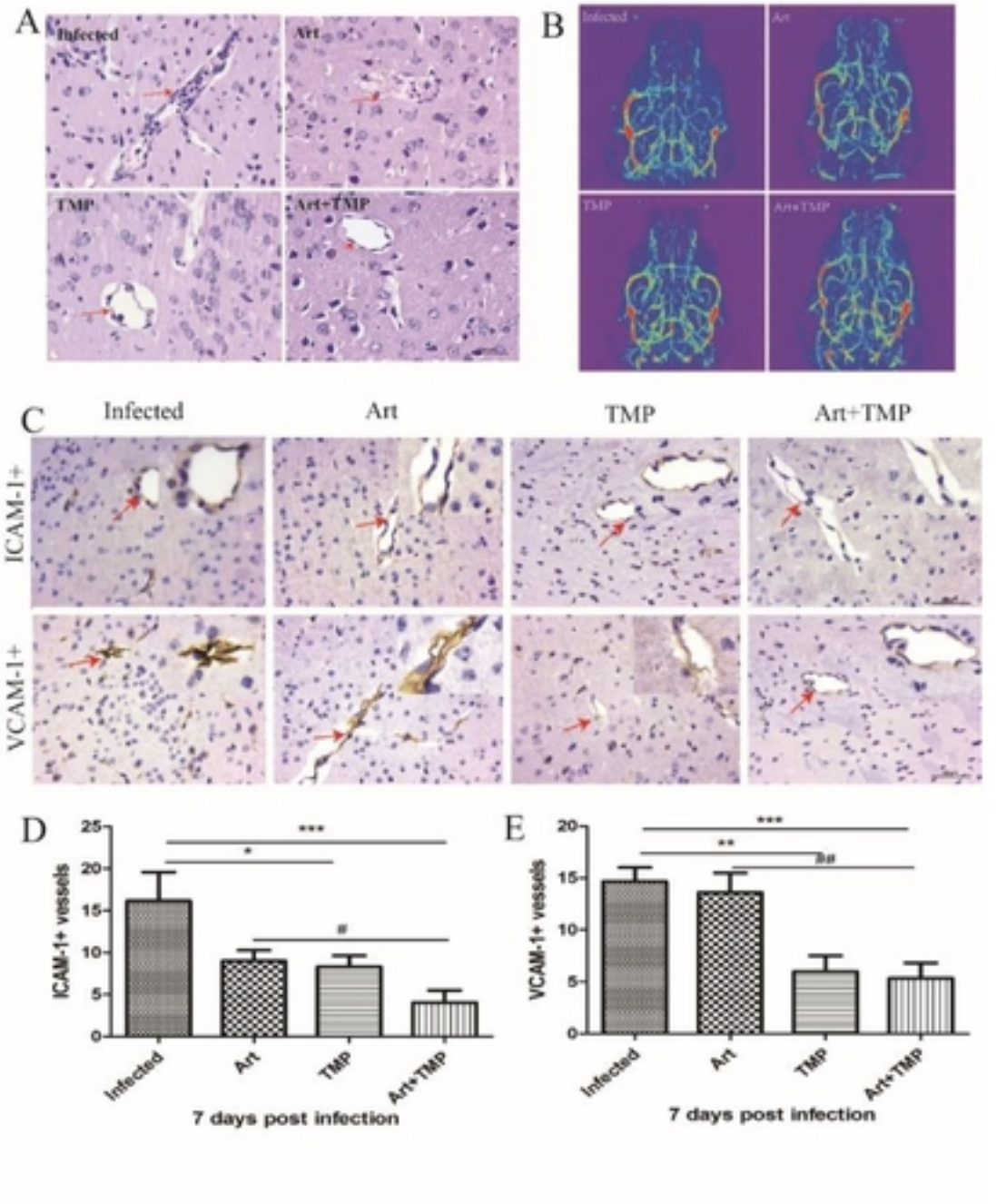
A
Infected
Art
TMP
Art+TMP
B
C
Infected
Art
TMP
Art+TMP
ICAM-1+
VCAM-1+
D
ICAM-1+ vessels
25
20
15
10
5
0
***
*
#
Infected
Art
TMP
Art+TMP
7 days post infection
E
VCAM-1+ vessels
20
15
10
5
0
***
**
##
Infected
Art
TMP
Art+TMP
7 days post infection

Fig.5

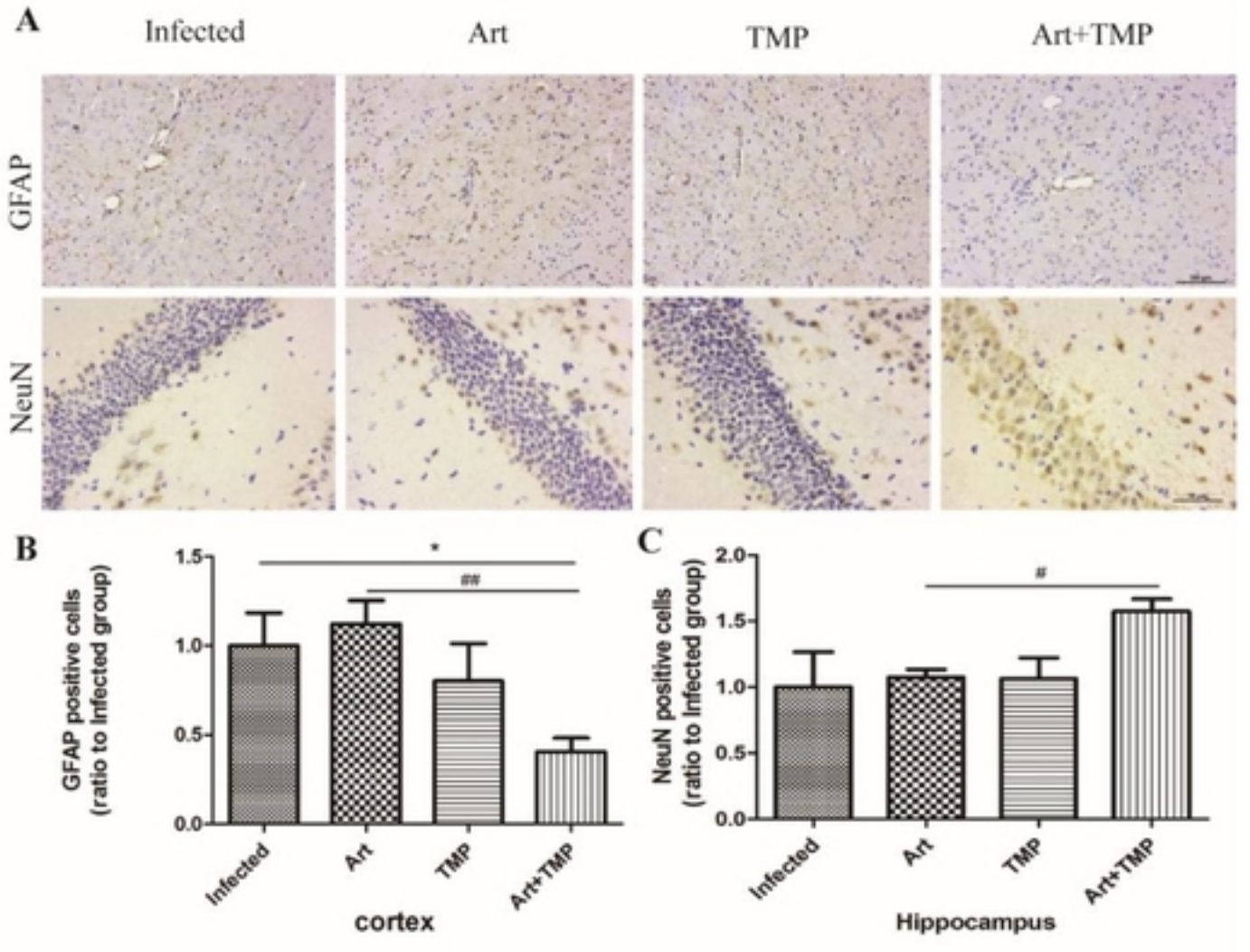
A
Infected
Art
TMP
Art+TMP
GFAP
NeuN
B
GFAP positive cells
(ratio to Infected group)
1.5
1.0
0.5
0.0
*
##
Infected
Art
TMP
Art+TMP
cortex
C
NeuN positive cells
(ratio to Infected group)
2.0
1.5
1.0
0.5
0.0
#
Infected
Art
TMP
Art+TMP
Hippocampus

Fig.6

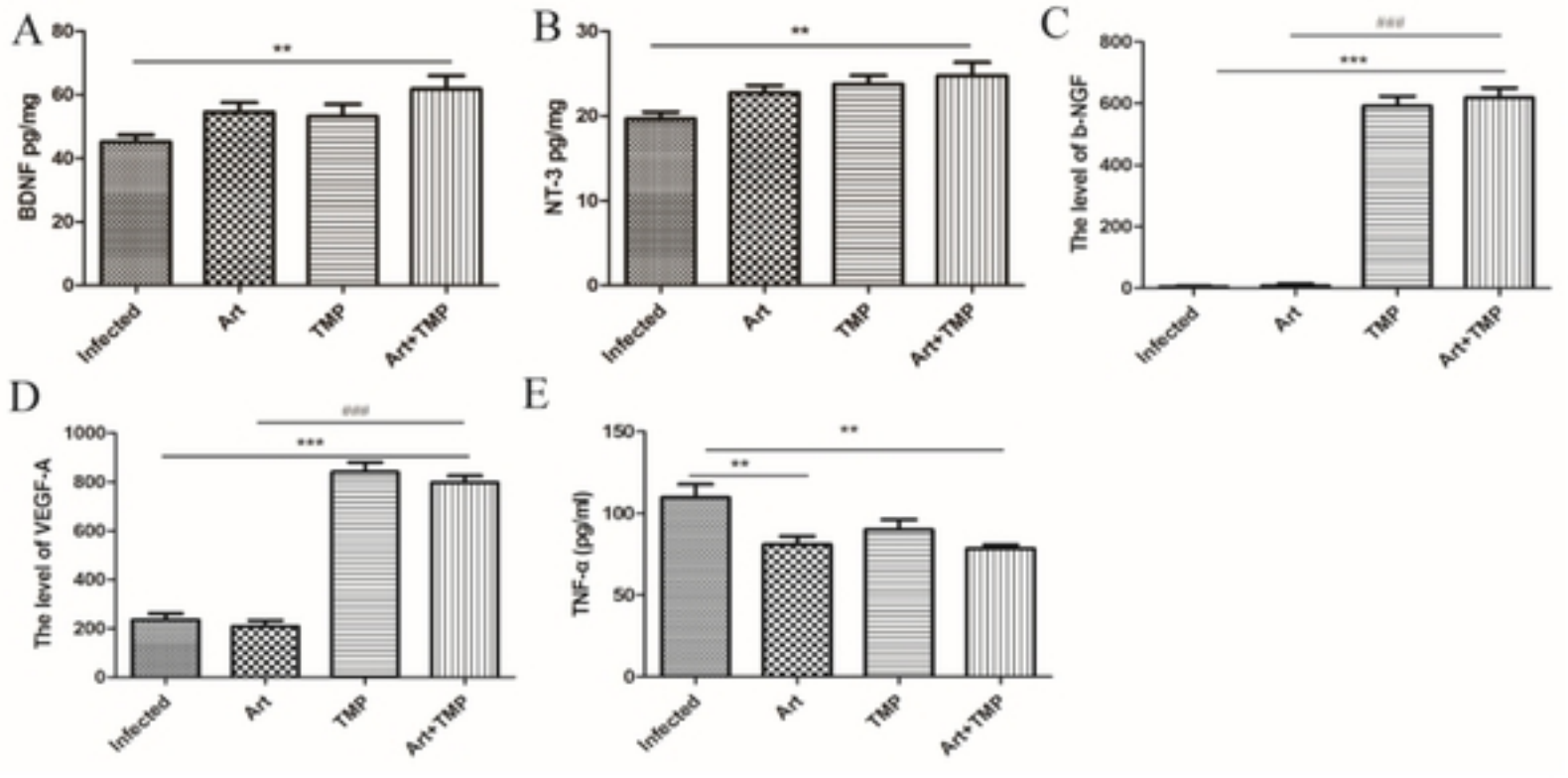
A
BDNF pg/mg
80
60
40
20
0
**
Infected
Art
TMP
Art+TMP
B
NT-3 pg/mg
30
20
10
0
**
Infected
Art
TMP
Art+TMP
C
The level of b-NGF
800
600
400
200
0
###
***
Infected
Art
TMP
Art+TMP
D
The level of VEGF-A
1000
800
600
400
200
0
###
***
Infected
Art
TMP
Art+TMP
E
TNF-α (pg/ml)
150
100
50
0
**
**
Infected
Art
TMP
Art+TMP

Fig.7

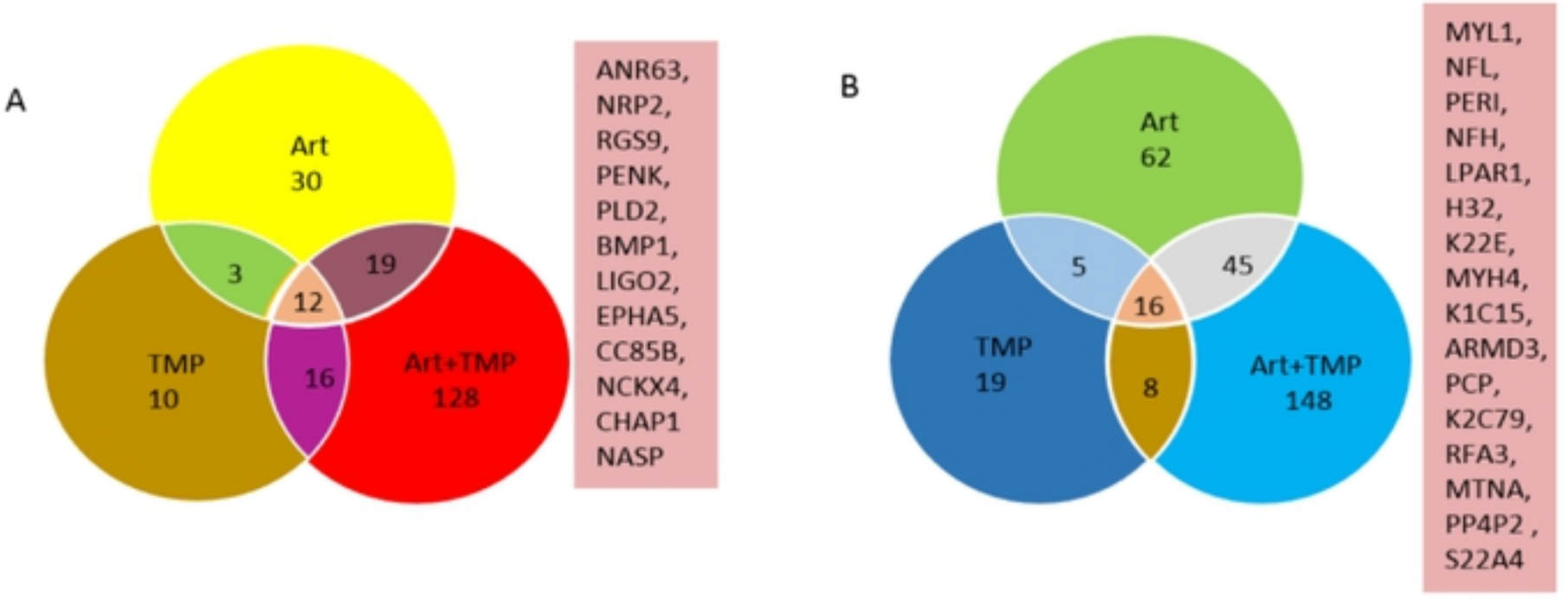
A
Art
30
3
19
12
TMP
10
16
Art+TMP
128
ANR63,
NRP2,
RGS9,
PENK,
PLD2,
BMP1,
LIGO2,
EPHA5,
CC85B,
NCKX4,
CHAP1
NASP
B
Art
62
5
45
16
TMP
19
8
Art+TMP
148
MYL1,
NFL,
PERI,
NFH,
LPAR1,
H32,
K22E,
MYH4,
K1C15,
ARMD3,
PCP,
K2C79,
RFA3,
MTNA,
PP4P2 ,
S22A4

C

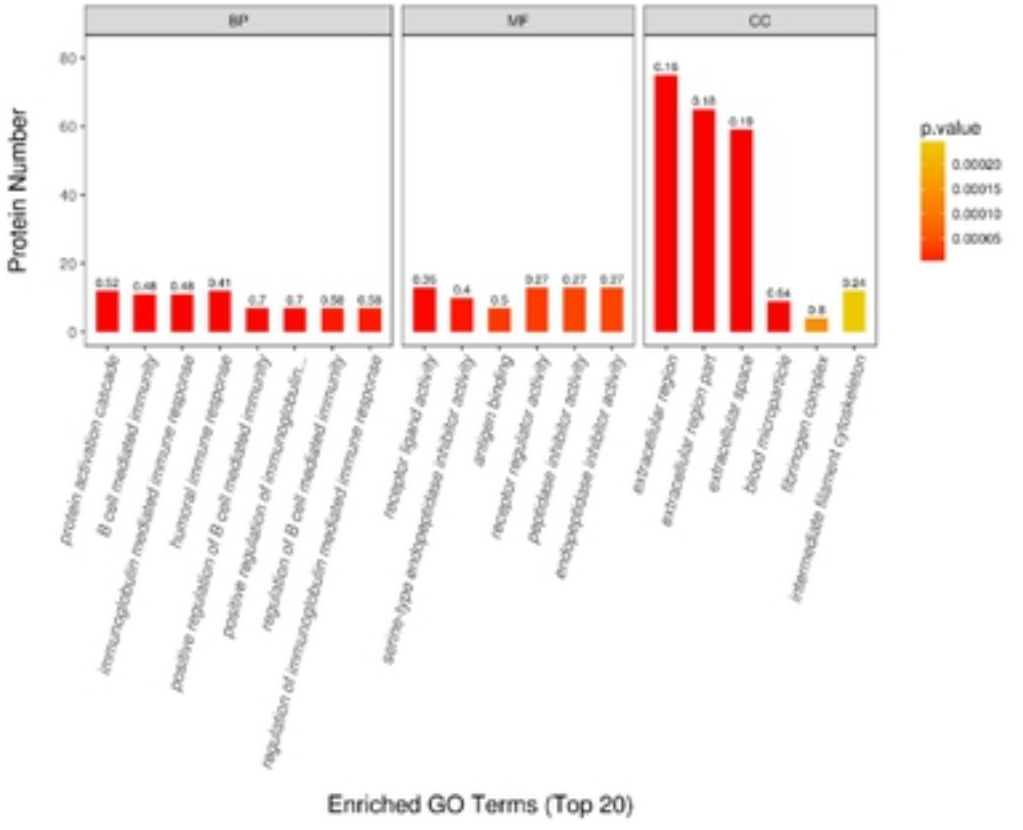
BP
MF
CC
Protein Number
0
20
40
60
80
0.52
0.48
0.48
0.41
0.7
0.7
0.58
0.58
0.36
0.4
0.5
0.27
0.27
0.27
0.78
0.65
0.6
0.64
0.8
0.24
protein activation cascade
B cell mediated immunity
immunoglobulin mediated immune response
humoral immune response
positive regulation of B cell mediated immunity
positive regulation of immunoglobulin...
regulation of B cell mediated immunity
regulation of immunoglobulin mediated immune response
receptor ligand activity
serine-type endopeptidase inhibitor activity
antigen binding
receptor regulator activity
peptidase inhibitor activity
endopeptidase inhibitor activity
extracellular region
extracellular region part
extracellular space
blood microparticle
fibrinogen complex
intermediate filament cytoskeleton
p.value
0.00020
0.00015
0.00010
0.00005
Enriched GO Terms (Top 20)

D

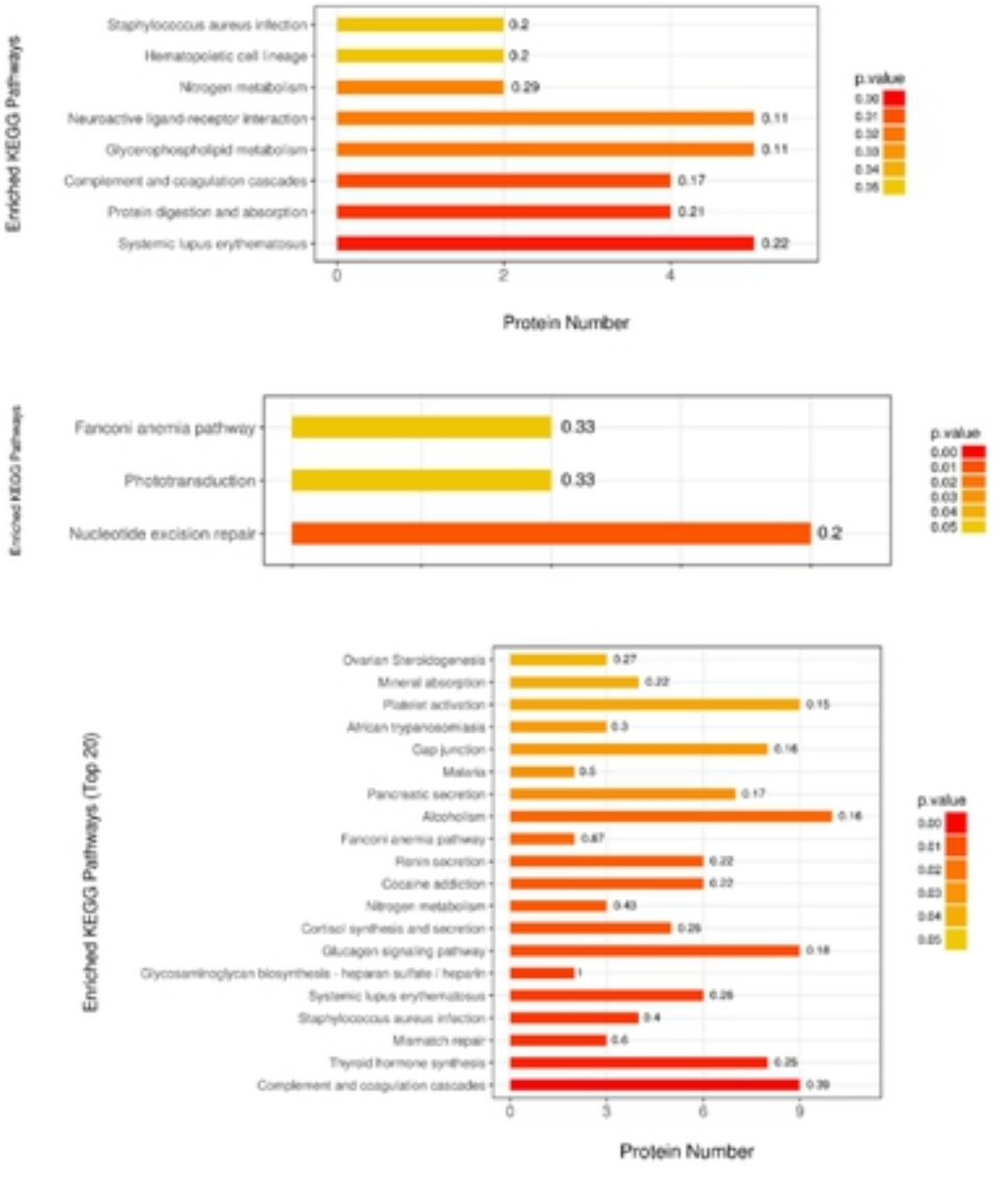
Enriched KEGG Pathways
Staphylococcus aureus infection
Hematopoietic cell lineage
Nitrogen metabolism
Neuroactive ligand-receptor interaction
Glycerophospholipid metabolism
Complement and coagulation cascades
Protein digestion and absorption
Systemic lupus erythematosus
0.2
0.2
0.29
0.11
0.11
0.17
0.21
0.22
0
2
4
Protein Number
p.value
0.30
0.31
0.32
0.33
0.34
0.35
Enriched KEGG Pathways
Fanconi anemia pathway
Phototransduction
Nucleotide excision repair
0.33
0.33
0.2
p.value
0.00
0.01
0.02
0.03
0.04
0.05
Enriched KEGG Pathways (Top 20)
Ovarian Steroidogenesis
Mineral absorption
Platelet activation
African trypanosomiasis
Gap junction
Malaria
Pancreatic secretion
Alcoholism
Fanconi anemia pathway
Renin secretion
Cocaine addiction
Nitrogen metabolism
Cortisol synthesis and secretion
Glucagon signaling pathway
Glycosaminoglycan biosynthesis - heparan sulfate / heparin
Systemic lupus erythematosus
Staphylococcus aureus infection
Mismatch repair
Thyroid hormone synthesis
Complement and coagulation cascades
0.27
0.22
0.15
0.3
0.16
0.5
0.17
0.18
0.67
0.22
0.22
0.40
0.26
0.18
1
0.26
0.4
0.6
0.25
0.39
0
3
6
9
Protein Number
p.value
0.00
0.01
0.02
0.03
0.04
0.05

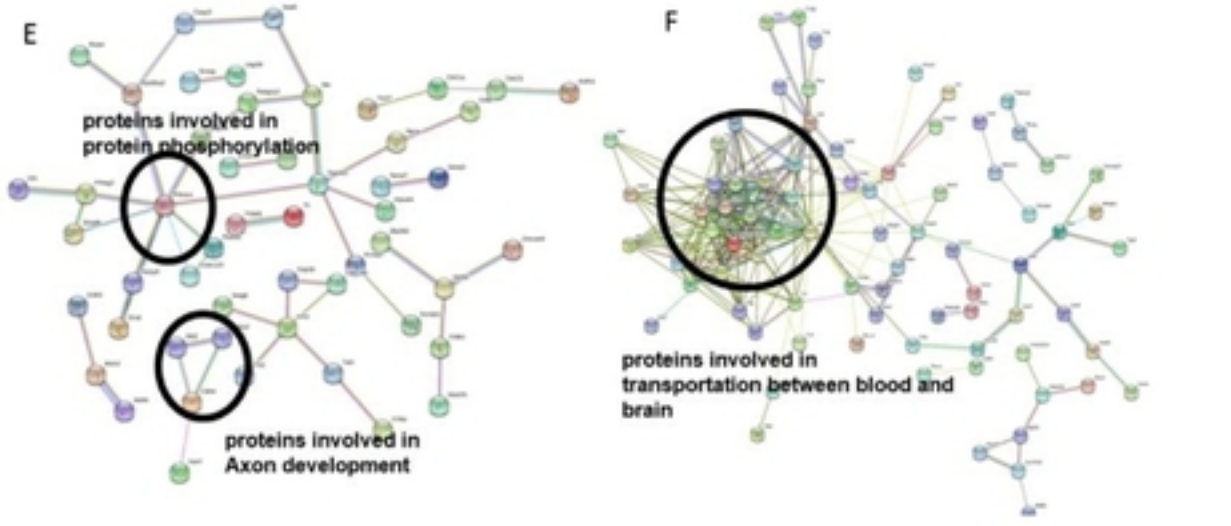
E
proteins involved in
protein phosphorylation
proteins involved in
Axon development
F
proteins involved in
transportation between blood and
brain

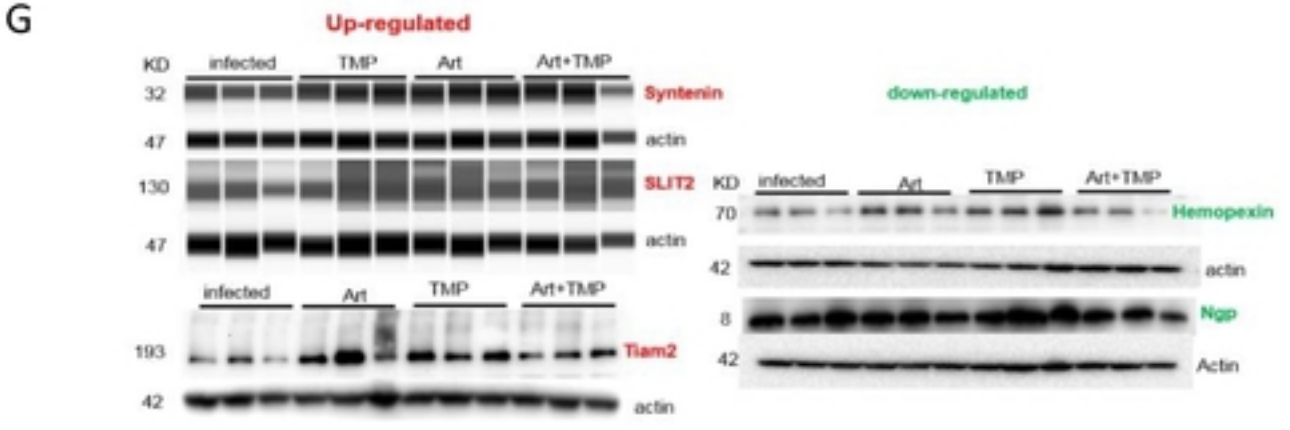
G
Up-regulated
KD
infected
TMP
Art
Art+TMP
32
Syntenin
47
actin
130
SLIT2
47
actin
infected
Art
TMP
Art+TMP
193
Tiam2
42
actin
down-regulated
KD
infected
Art
TMP
Art+TMP
70
Hemopexin
42
actin
8
Ngp
42
Actin

Fig.8